An extension of a high order approach for free vibration analysis of the nano-scale sandwich beam with steel skins for two types of soft and stiff cores

S. Masoud Marandi [a], Mohsen Botshekanan Dehkordi [*] and S. Hassan Nourbakhsh [b]

Faculty of Engineering, Shahrekord University, Shahrekord, Iran

Abstract. The study investigates the free vibration of a nano-scale sandwich beam by an extended high order approach, which has not been reported in the existing literature. First-order shear deformation theory for steel skins and so-called high-order sandwich panel theory for the core are applied. Next, the modified couple stress theory is used for both skins and cores. The Hamilton principle is utilized for deriving equations and corresponding boundary conditions. First, in the study the three-mode shapes natural frequencies for various material parameters are investigated. Also, obtained results are evaluated for two types of stiff and soft cores and isotropic, homogenous steel skins. In the research since the governing equations and also the boundary conditions are nonhomogeneous, therefore some closed-form solutions are not applicable. So, to obtain natural frequencies, the boundary conditions are converted to initial conditions called the shooting method as the numerical one. This method is one of the most robust approaches to solve complex equations and boundary conditions. Moreover, three types of simply supported on both sides of the beam (S-S), simply on one side and clamp supported on the other one (S-C) and clamped supported on both sides (C-C) are scrutinized. The parametric study is followed to evaluate the effect of nano-size scale, geometrical configurations for skins, core and material property change for cores as well. Results show that natural frequencies increase by an increase in skins thickness and core Young modulus and a decrease in beam length, core thickness as well. Furthermore, differences between obtained frequencies for soft and stiff cores increase in higher mode shapes; while, the more differences are evaluated for the stiff one.

Keywords: shooting method; modified couple stress theory; free vibration; nano-scale sandwich beam

1. Introduction

Sandwich structures can be classed as composite materials in that they consist of two or more individual components of differing properties, which, when combined, result in a high-performance material. Amongst all possible design concepts in composite structures, the idea of sandwich construction has become increasingly popular because of the development of human-made cellular materials that are used as core materials.

The separation of the skins by the core increases the moment of inertia of the beam with little increase in weight, which produce an efficient structure for resisting bending and buckling loads. Sandwich beams are popular in high performance applications where weight must be kept to a minimum; for example, they are popular in aeronautical structures, high-speed marine craft and racing cars.

In the most weight-critical applications, composite materials are used for the skins; cheaper alternatives such as aluminum alloy, steel or plywood are also commonly used.

Materials used for cores include polymers, aluminum, wood and composites. To minimize weight, these composite materials are used in the form of foams, honeycombs or with a corrugated construction.

Usually a sandwich structure consists of two relatively thin, stiff and strong faces separated by a relatively thick lightweight core, such as, honeycomb, balsa or foam cores. The purpose of a sandwich structure is to achieve a stiff and simultaneously light component.

Sandwich theory describes the behavior of a beam, plate or shell that consists of three layers -two face sheets and one core. The most commonly used sandwich theory is classical, in which the core is vertically incompressible. In other words, longitudinal stress through the core is neglected (Vinson 1999). The free vibration examination of the FG [1] sandwich beam by the mesh-free method is reported by Yang *et al.* (2014). The high-order sandwich panel theory in which compatibility conditions between two face sheets and the core are used is introduced as the so-called Model II (Frostig *et al.* 1992).

The free vibration and nonlinear thermal response of the sandwich beam with a soft core are examined in works by Frostig and Thomsen (2009). The effects of CNT [2] length and CNT-matrix interphase in carbon nanotube

---

∗Corresponding author, Ph.D.,
 E-mail: mbd_dehkordi@yahoo.com
[a] Ph.D. Student, E-mail: marandi1362@gmail.com
[b] Ph.D., E-mail: shassanns@yahoo.com

[1] Functionally graded
[2] Carbon nanotube

reinforced composites is assessed by (Wan *et al.* 2005). Non-linear dynamic response of a single wall carbon nanotube subjected to radial impulse is explored by Dai and Wang (2006). The dynamic stiffness method is used to scrutinize the free vibration of the sandwich beam with a soft core by Damanpack and Khalili (2012). Efficiency of reinforcement in composite structures is determined by Loos and Manas-Zloczower (2012). Numerical analysis on nonlinear free vibration of carbon nanotube reinforced composite beams is studied by Lin and Xiang (2014). Nonlinear dynamics of the piezoelectric nanocomposite under parametric resonance is scrutinized by He *et al.* (2015).

New high-order theory for obtaining the free vibration and buckling of the sandwich beam is performed by Nguyen *et al.* (2015). Free vibration of the sandwich beam with functionally graded syntactic soft core is studied by Rahmani *et al.* (2009). Panel flutter characteristics of sandwich plates with CNT reinforced face sheets using an accurate higher-order theory is performed by Sankar *et al.* (2014). Effect of agglomeration on the natural frequencies of functionally graded carbon nanotube-reinforced laminated composite doubly-curved shells is determined by Tornabene *et al.* (2016). Application of Reddy's third-order theory to delaminated orthotropic composite plates is applied by Szekrényes (2014).

Nonlinear vibration analysis of composite laminated and sandwich plates with random material properties is done by Chandrashekhar and Ganguli (2010). Free vibration of functionally graded sandwich plates using four-variable refined plate theory is surveyed by Hadji *et al.* (2011). Static behavior of viscoelastic sandwich plate with nanocomposite facings under mechanical load is fulfilled by Kavalur *et al.* (2014). Large deformation bending analysis of functionally graded spherical shell using FEM[3] is assessed by Kar and Panda (2015). Experimental snap-buckling behavior of thin GRP[4] curved panel under lateral loading is accomplished by Marshall *et al.* (1977). Free vibration analysis of functionally graded conical shells and annular plates using the Haar wavelet method is examined by Xie *et al.* 2014).

3-D free vibration analysis of FG-multiwalled CNT curved sandwich panel with power law distribution of carbon nanotubes is fulfilled by Tahouneh (2017). In the study, mode shapes of FG-MWCNT[5] sandwich panel are obtained as well. Free vibration of magneto-thermo-mechanical viscoelastic curved microbeam reinforced by functionally graded carbon nanotubes is performed by Allahkarami *et al.* (2017). A microbeam resting on a viscoelastic medium and equations and boundary conditions obtained by using strain gradient and Timoshenko beam theories are all studied in the evaluation.

Tagrara *et al.* (2015) performed bending, buckling and free vibration of FG-CNT beam resting on an elastic foundation by using a trigonometric refined theory that deals with three unknowns. Bending response of the functionally graded carbon nanotube plate is implemented

by Chavan and Lal (2017). In the work, high-order shear deformation and finite element methods are used for obtaining equations and boundary conditions and solving them, respectively. A new hyperbolic beam theory is applied in order to obtain free vibration and buckling of the FG-CNT sandwich beam by Bennai *et al.* (2015). In the study, the core layer is considered to be a homogenous and isotropic material. An analytical method is used in the study for considering a simply supported boundary condition to obtain buckling and free vibration.

The benchmark solution for free vibration of functionally graded moderately thick annular sector plates is investigated by Saidi *et al.* (2011). Free vibration of polar orthotropic laminated circular and annular plates is obtained by Lin and Tseng (1998). Asymmetric free vibrations of laminated annular cross-ply circular plates including the effects of shear deformation and rotary inertia is studied by Viswanathan *et al.* (2009). An improved Fourier series solution for the dynamic analysis of laminated composite annular, circular, and sector plate with general boundary conditions is surveyed by Wang *et al.* (2016). A novel nonlocal gradient formulation is utilized for the functionally graded Timoshenko nanobeams by Barretta *et al.* (2016). Free vibration of laminated conical shells including transverse shear deformation is scrutinized by Tong (1994).

Dynamic properties of the sandwich beam with reinforced various layers of carbon epoxy polymer composites used for face sheets and lightweight concrete for core layer is implemented by Naghipour and Mehrzadi (2007). Free vibration analysis of circular thin plates with stepped thickness by the DSC[6] element method is accomplished by Duan *et al.* (2014). Forced vibration analysis of FG-CNT sandwich plate is examined by Ansari *et al.* (2014) who concluded that bending stiffness and natural frequency increase by growth in volume fraction of CNT face sheets. Large deflection analysis of laminated composite plates resting on nonlinear elastic foundations by the method of discrete singular convolution is examined in work of Baltacıoğlu *et al.* (2011).

Free vibration of thick FG-CNT plate resting on the elastic foundation is evaluated by Zhang *et al.* (2015). The free vibration and buckling of sandwich beam with FG-CNT face sheets and Ti-6Al-4V stiff core are examined by Wu *et al.* (2015). The effect of elevated temperature on free vibration of FG-CNT plate is investigated by Mehar *et al.* (2016). Nonlinear free vibration and nonlinear bending of sandwich plates with CNT face sheets resting on Pasternak foundation is found in work of Wang and Shen (2012).

Post-buckling behavior of the sandwich plate with CNT face sheets resting on Pasternak foundation is studied by Shen and Zhu (2012) who concluded that post-buckling behavior of the sandwich plate is affected by temperature change, volume fraction of face sheets, and core to face sheet thickness ratio. An effect of carbon nanotubes existence on the vibration of CNT reinforced beam is fulfilled by Heshmati *et al.* (2015). In the work, effect of factors such as length, agglomeration, waviness and distribution of carbon nanotubes on the vibration of FG-

---

[3] Finite element method
[4] Glass-reinforced plastic
[5] Multiwalled CNT

[6] Discrete singular convolution

CNT beams are scrutinized. The discrete singular convolution technique is used to obtain the free vibration of symmetric laminated skew plates by the first-order shear deformation theory is studied in work of Gürses *et al.* (Gürses *et al.* 2009). The free vibration of curved nano-scale beam by nonlocal theory is evaluated by Ganapathi *et al.* (2018). In the work, the finite element method is used for obtaining natural frequencies. Moreover, the effect of beam length, beam curvature, beam thickness and material parameters on frequency values is investigated.

In this paper, the free vibration analysis of the nano-scale sandwich beam by an extended high order approach including two types of soft and stiff cores is evaluated. In our study, the first-order shear deformation displacement fields are used for isotropic, homogenous, and steel face sheets and displacement fields of cores is derived by HSAPT[7]. MCST[8] is then applied for both skins and the core. The Hamilton principle is utilized for deriving equations and corresponding boundary conditions. Then, the shooting method, as a numerical method, is used to obtain natural frequency by considering three types of S-S, S-C and C-C boundary conditions. Our paper novelty is that both theories, HSAPT and MCST, are applied for the core, which has not been reported in the literature thus far.

2. Mathematical approach

The modified couple stress theory is used for obtaining equations and corresponding boundary conditions. The theory consists of classical term and the nonclassical terms, which allude to micro/nano-scale mechanical elements whose size is in order of micron or nano such as micro/nano sandwich beams as discussed in the paper. It is proven that the deformation of such systems is size dependent, which is why material length scale parameters in the modified couple stress theory applies (McFarland and Colton 2005). The theory is expressed as (Eq. (1)) (Asghari *et al.* 2010, Kahrobaiyan *et al.* 2011)

$$\delta U = \int_V (\sigma_{ij}\delta\varepsilon_{ij} + m_{ij}\delta\chi_{ij})dV = \delta U_s + \delta U_c = \int_{V_t} (\sigma_{ij}\delta\varepsilon_{ij} + m_{ij}\delta\chi_{ij})dV_t +$$
$$\int_{V_b} (\sigma_{ij}\delta\varepsilon_{ij} + m_{ij}\delta\chi_{ij})dV_b + \int_{V_c} (\sigma_{ij}\delta\varepsilon_{ij} + m_{ij}\delta\chi_{ij})dV_c \tag{1}$$

In the above equation, δU_s, δU_c, u_i, ω_i, ε_{ij}, σ_{ij} and χ_{ij} denote skins and core strain energy variations, the displacement vector, rotation vector, strain and stress tensor, and symmetric part of rotation gradient tensor components, respectively and is written as

$$\omega_i = \frac{1}{2}(curl(u))_i \tag{2}$$

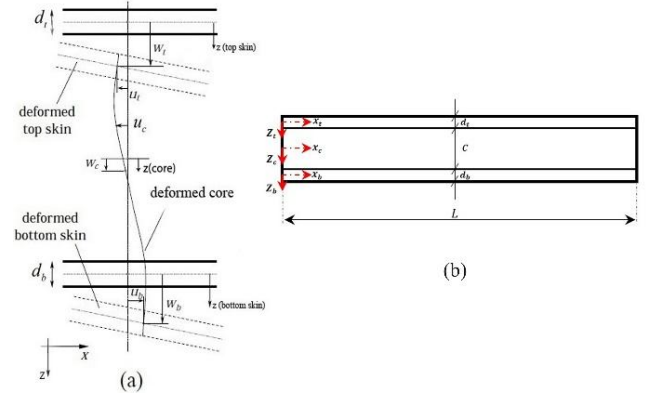$$\varepsilon_{ij} = \frac{1}{2}(\frac{\partial u_i}{\partial x_j} + \frac{\partial u_j}{\partial x_i}) \tag{3}$$

Fig. 1 A schematic view of deformed sandwich beam: (a) Deformations; (b) Sandwich beam

$$\sigma_{ij} = \lambda tr(\varepsilon)\delta_{ij} + 2\mu\varepsilon_{ij} \tag{4}$$

$$\chi_{ij} = \frac{1}{2}(\frac{\partial \omega_i}{\partial x_j} + \frac{\partial \omega_j}{\partial x_i}) \tag{5}$$

So-called high-order stress in Eq. (1) is expressed as

$$m_{ij} = 2\mu l^2 \chi_{ij} \tag{6}$$

λ, μ and l are the Lame constants and material length scale parameter, respectively. Equations and boundary conditions are derived by using the variational calculus concept or Hamilton's principle (Eq. (7)). Displacement fields for face sheets are considered as Timoshenko beam theory which has the following form (Eq. (8)). Also, Eq. (13) represents longitudinal and transverse deformations of the core and are expressed in the form of HSAPT or Model II of FROSTIG (Frostig *et al.* 1992). A schematic of a deformed sandwich beam is depicted in Fig. 1.

$$\delta \int_{t_1}^{t_2} (T - U)dt = 0 \tag{7}$$

$$\begin{cases} u_i(x,z,t) = u_{0i}(x,t) + z_i\phi_i(x,t) \\ v_i(y,z,t) = 0 \\ w_i(x,z,t) = w_i(x,t) \end{cases} \tag{8}$$

$$\begin{cases} u_c(x,z,t) = \\ \quad u_0(x,t) + u_1(x,t)z_c + u_2(x,t)z_c^2 + u_3(x,t)z_c^3 \\ w_c(x,z,t) = \\ \quad w_0(x,t) + w_1(x,t)z_c + w_2(x,t)z_c^2 \end{cases} \tag{9}$$

First, for keeping continuity between the core and two layers, compatibility conditions written in Eq. (10) are exerted.

---

[7] High-order sandwich panel theory
[8] The modified couple stress theory

$$\begin{cases} w_c(x, -\frac{c}{2}, t) = w_t(x, z, t) \\ u_c(x, -\frac{c}{2}, t) = u_{0t}(x, t) + \frac{d_t}{2}\phi_t(x, t) \\ w_c(x, \frac{c}{2}, t) = w_b(x, z, t) \\ u_c(x, \frac{c}{2}, t) = u_{0b}(x, t) - \frac{d_b}{2}\phi_b(x, t) \end{cases} \quad (10)$$

Next, longitudinal and transverse deformations of the core by incorporating Eq. (10) into Eq. (9) are rewritten as

$$\begin{cases} u_c(x, z, t) = \\ \quad u_0(x, t) + u_1(x, t)z_c + \frac{2}{c^2}[u_{0t}(x, t) + u_{0b}(x, t) - 2u_0(x, t) \\ \quad + \frac{d_t}{2}\phi_t(x, t) - \frac{d_b}{2}\phi_b(x, t)]z_c^2 + \frac{4}{c^3}[-u_{0t}(x, t) - \frac{d_t}{2}\phi_t(x, t) \\ \quad - \frac{d_b}{2}\phi_b(x, t) - cu_1(x, t)]z_c^3 \\ w_c(x, z, t) = \\ \quad w_0(x, t) + \frac{1}{c}[w_b(x, t) - w_t(x, t)]z_c + \frac{2}{c^2}[w_t(x, t) \\ \quad - w_b(x, t) - 2w_0(x, t)]z_c^2 \end{cases} \quad (11)$$

3. Governing equations and boundary conditions

In this section, equations and corresponding boundary conditions of the nano-scale sandwich beam are obtained by using MCST. The strain of the top and bottom skins is gained from the displacement fields, Eq. (8), as following (Eq. (12)).

$$\begin{cases} \varepsilon_{xx}^i(x, z, t) = \frac{\partial u_{0i}(x, t)}{\partial x} + z_i \frac{\partial \phi_i(x, t)}{\partial x} \\ \gamma_{xz}^i(x, z, t) = \phi_i(x, t) + \frac{\partial w_i(x, t)}{\partial x} \end{cases}, i = t, b \quad (12)$$

Skins (top and bottom layers) strain energy is therefore written in the form of Eq. (13).

$$\delta U_s = \\ \int_{V_t}(\sigma_{xx}^t\delta\varepsilon_{xx}^t + k_s\tau_{xz}^t\delta\gamma_{xz}^t + m_{12}^t\delta\chi_{12}^t + m_{21}^t\delta\chi_{21}^t)dV_t \\ + \int_{V_b}(\sigma_{xx}^b\delta\varepsilon_{xx}^b + k_s\tau_{xz}^b\delta\gamma_{xz}^b + m_{12}^b\delta\chi_{12}^b + m_{21}^b\delta\chi_{21}^b)dV_b \quad (13)$$

In Eq. (13), the shear correction factor, k_S, is considered as $\frac{\pi^2}{12}$ (Ansari *et al.* 2014). Moreover, symmetric part of rotation gradient tensor components and high-order stress for skins are

$$\begin{cases} \chi_{12}^i = \chi_{21}^i = \frac{1}{4}(\frac{\partial\phi_i(x, t)}{\partial x} - \frac{\partial^2 w_i(x, t)}{\partial x^2}) \\ m_{12}^i = m_{21}^i = \frac{1}{2}\mu_i l^2(\frac{\partial\phi_i(x, t)}{\partial x} - \frac{\partial^2 w_i(x, t)}{\partial x^2}) \end{cases} i = t, b \quad (14)$$

Also the variation of skins kinetic energy turns into Eq. (15).

$$\delta T_s = \int_0^t \{\int_0^l [-m_t(\frac{d_t^2}{12}\ddot{\phi}_t\delta\phi_t + \ddot{u}_{0t}\delta u_{0t} + \ddot{w}_t\delta w_t) \\ - m_b(\frac{d_b^2}{12}\ddot{\phi}_b\delta\phi_b + \ddot{u}_{0b}\delta u_{0b} + \ddot{w}_b\delta w_b)]dx\}dt \quad (15)$$

In the above equation, $\ddot{}$ is second derivation with respect to time.

In this step, strain and kinetic variations of the core are derived.

Strains of the core regarding displacement fields, Eq. (11), are given in Eq. (16) as well.

$$\begin{cases} \varepsilon_{zz}^c = \frac{1}{c}[w_b(x, t) - w_t(x, t)] + \frac{4}{c^2}[w_t(x, t) - w_b(x, t) - 2w_0(x, t)]z_c \\ \varepsilon_{xx}^c = (1 - \frac{4z_c^2}{c^2})\frac{\partial u_0(x, t)}{\partial x} + (z_c - \frac{4z_c^3}{c^2})\frac{\partial u_1(x, t)}{\partial x} + \frac{2z_c^2}{c^2}(1 - \frac{2z_c}{c})\frac{\partial u_{0t}(x, t)}{\partial x} \\ \quad + \frac{2z_c^2}{c^2}(1 + \frac{2z_c}{c})\frac{\partial u_{0b}(x, t)}{\partial x} + \frac{z_c^2 d_t}{c^2}(1 - \frac{2z_c}{c})\frac{\partial\phi_t(x, t)}{\partial x} + \\ \quad \frac{z_c^2 d_b}{c^2}(-1 - \frac{2z_c}{c})\frac{\partial\phi_b(x, t)}{\partial x} \\ \gamma_{xz}^c = u_1(x, t) + \frac{4}{c^2}[u_{0t}(x, t) + u_{0b}(x, t) - 2u_0(x, t) \\ \quad + \frac{d_t}{2}\phi_t(x, t) - \frac{d_b}{2}\phi_b(x, t)]z_c + \frac{12}{c^3}[-u_{0t}(x, t) - \frac{d_t}{2}\phi_t(x, t) - \\ \quad \frac{d_b}{2}\phi_b(x, t) - cu_1(x, t)]z_c^2 + \frac{\partial w_0(x, t)}{\partial x} + \frac{z_c}{c}[\frac{\partial w_b(x, t)}{\partial x} - \frac{\partial w_t(x, t)}{\partial x}] \\ \quad + \frac{2z_c^2}{c^2}[\frac{\partial w_t(x, t)}{\partial x} - \frac{\partial w_b(x, t)}{\partial x} - 2\frac{\partial w_0(x, t)}{\partial x}] \end{cases} \quad (16)$$

Strain energy variation of the core becomes

$$\int_{V_c}\begin{pmatrix} \sigma_{xx}^c\delta\varepsilon_{xx}^c + \sigma_{zz}^c\delta\varepsilon_{zz}^c + \tau_{xz}^c\delta\gamma_{xz}^c + m_{12}^c\delta\chi_{12}^c + m_{21}^c\delta\chi_{21}^c + m_{23}^c\delta\chi_{23}^c + \\ m_{32}^c\delta\chi_{32}^c \end{pmatrix}dV_c \quad (17)$$

In Eq. (17), symmetric part of rotation gradient tensor components and high-order stress of the core are

$$\begin{cases} \chi_{12}^c = (\frac{\partial^2 u_c(x, z, t)}{\partial x\partial z} - \frac{\partial^2 w_c(x, z, t)}{\partial x^2}) = \chi_{21}^c \\ m_{12}^c = 2\mu_c l^2(\frac{\partial^2 u_c(x, z, t)}{\partial x\partial z} - \frac{\partial^2 w_c(x, z, t)}{\partial x^2}) = m_{21}^c \\ \chi_{23}^c = (\frac{\partial^2 u_c(x, z, t)}{\partial z^2} - \frac{\partial^2 w_c(x, z, t)}{\partial x\partial z}) = \chi_{32}^c \\ m_{23}^c = 2\mu_c l^2(\frac{\partial^2 u_c(x, z, t)}{\partial z^2} - \frac{\partial^2 w_c(x, z, t)}{\partial x\partial z}) = m_{32}^c \end{cases} \quad (18)$$

Also Eq. (19) represents the kinetic energy variation of the core.

$$\delta T_c = \delta\{\int_{V_c}\frac{1}{2}\rho_c(\dot{u}_c^2 + \dot{w}_c^2)dV_c\} \quad (19)$$

In Eq. (19), $\dot{}$ is first derivation with respect to time. By substituting u_c and w_c from Eq. (11) into Eq. (19) and after some cumbersome algebraic manipulation, variation of

kinetic energy of the core is obtained.

By incorporating Eqs. (13) and (15) for face sheets and Eqs. (17) and (19) for the core into Eq. (7), followed by cumbersome and time-consuming manipulation and using integration by parts, the equations and corresponding boundary conditions are extracted.

Equations of motion of nano-scale sandwich beam are

$$\delta u_{0t}: \frac{1}{15}m_c\frac{\partial^2}{\partial t^2}u_0(x,t)+\frac{m_c}{70}\frac{\partial^2}{\partial t^2}u_{0b}(x,t)-\frac{m_c d_b}{140}\frac{\partial^2}{\partial t^2}\phi_b(x,t)$$

$$-\frac{m_c c}{70}\frac{\partial^2}{\partial t^2}u_1(x,t)-\frac{7bG_c u_{0b}(x,t)}{15c}-\frac{8}{3}\frac{bG_c u_0(x,t)}{c}-$$

$$\frac{E_c bc}{70-70v_c^2}\frac{\partial^2}{\partial x^2}u_{0b}(x,t)-\frac{1}{15}\frac{E_c bc}{1-v_c^2}\frac{\partial^2}{\partial x^2}u_0(x,t)+m_t\frac{\partial^2}{\partial t^2}u_{0t}(x,t)$$

$$+\frac{3m_c}{35}\frac{\partial^2}{\partial t^2}u_{0t}(x,t)\frac{E_c bc^2}{70-70v_c^2}\frac{\partial^2}{\partial x^2}u_1(x,t)+\frac{E_c bcd_b}{140-140v_c^2}\frac{\partial^2}{\partial x^2}\phi_b(x,t)$$

$$+\frac{7bG_c d_b\phi_b(x,t)}{30c}+\frac{47bG_c d_t\phi_t(x,t)}{30c}-\frac{19G_c b}{30}\frac{\partial}{\partial x}w_t(x,t)+$$

$$\frac{11E_c bv_c}{30-30v_c^2}\frac{\partial}{\partial x}w_t(x,t)-\frac{3E_c bc}{35-35v_c^2}\frac{\partial^2}{\partial x^2}u_{0t}(x,t)-\frac{3E_c bcd_t}{70-70v_c^2}\frac{\partial^2}{\partial x^2}\phi_t(x,t)$$

$$+\frac{1}{30}\frac{E_c bv_c}{1-v_c^2}\frac{\partial}{\partial x}w_b(x,t)+\frac{1}{30}G_c b\frac{\partial}{\partial x}w_b(x,t)-\frac{2}{5}\frac{E_c bv_c}{1-v_c^2}\frac{\partial}{\partial x}w_0(x,t)$$

$$-\frac{2}{5}G_c b\frac{\partial}{\partial x}w_0(x,t)-E_t d_t\frac{\partial^2}{\partial t^2}u_{0t}(x,t)-E_t\frac{d_t^2}{4}\frac{\partial^2}{\partial x^2}\phi_t(x,t)+$$

$$\frac{4}{5}bG_c u_1(x,t)+\frac{3m_c d_t}{70}\frac{\partial^2}{\partial t^2}\phi_t(x,t)-\frac{47\mu_c bl^2 d_t}{30c}\frac{\partial^2}{\partial x^2}\phi_t(x,t)-$$

$$\frac{7\mu_c bl^2 d_b}{30c}\frac{\partial^2}{\partial x^2}\phi_b(x,t)-\frac{4}{5}\mu_c bl^2\frac{\partial^2}{\partial x^2}u_1(x,t)-32\frac{\mu_c bl^2 u_{0b}(x,t)}{c^3}+$$

$$48\frac{\mu_c bl^2 u_1(x,t)}{c^2}-32\frac{\mu_c bl^2 u_0(x,t)}{c^3}-16\frac{\mu_c bl^2}{c^2}\frac{\partial}{\partial x}w_0(x,t)+$$

$$\frac{1}{30}\mu_c bl^2\frac{\partial^3}{\partial x^3}w_b(x,t)-\frac{19\mu_c bl^2}{30}\frac{\partial^3}{\partial x^3}w_t(x,t)+12\frac{\mu_c bl^2}{c^2}\frac{\partial}{\partial x}w_t(x,t)$$

$$+64\frac{\mu_c bl^2 u_{0t}(x,t)}{c^3}+4\frac{\mu_c bl^2}{c^2}\frac{\partial}{\partial x}w_b(x,t)-\frac{47\mu_c bl^2}{15c}\frac{\partial^2}{\partial x^2}u_{0t}(x,t)+$$

$$\frac{7\mu_c bl^2}{15c}\frac{\partial^2}{\partial x^2}u_{0b}(x,t)+\frac{8}{3}\frac{\mu_c bl^2}{c}\frac{\partial^2}{\partial x^2}u_0(x,t)+16\frac{\mu_c bl^2 d_b\phi_b(x,t)}{c^3}+$$

$$32\frac{\mu_c bl^2 d_t\phi_t(x,t)}{c^3}-\frac{2}{5}\mu_c bl^2\frac{\partial^3}{\partial x^3}w_0(x,t)+\frac{47bG_c u_{0t}(x,t)}{15c}=0$$

(20)

$$\delta u_{0b}: \frac{m_c c}{70}\frac{\partial^2}{\partial t^2}u_1(x,t)+\frac{1}{15}m_c\frac{\partial^2}{\partial t^2}u_0(x,t)+\frac{3m_c}{35}\frac{\partial^2}{\partial t^2}u_{0b}(x,t)+$$

$$\frac{m_c}{70}\frac{\partial^2}{\partial t^2}u_{0t}(x,t)-\frac{7bG_c u_{0t}(x,t)}{15c}-\frac{1}{15}\frac{E_c bc}{1-v_c^2}\frac{\partial^2}{\partial x^2}u_0(x,t)-$$

$$\frac{E_c bc}{70-70v_c^2}\frac{\partial^2}{\partial x^2}u_{0t}(x,t)-\frac{4}{5}bG_c u_1(x,t)+m_b\frac{\partial^2}{\partial t^2}u_{0b}(x,t)$$

$$+\frac{47bG_c u_{0b}(x,t)}{15c}-\frac{8}{3}\frac{bG_c u_0(x,t)}{c}+\frac{19\mu_c bl^2}{30}\frac{\partial^3}{\partial x^3}w_b(x,t)$$

$$-\frac{3m_c d_b}{70}\frac{\partial^2}{\partial t^2}\phi_b(x,t)-\frac{E_c bc^2}{70-70v_c^2}\frac{\partial^2}{\partial x^2}u_1(x,t)-\frac{E_c bcd_t}{140-140v_c^2}\frac{\partial^2}{\partial x^2}\phi_t(x,t)$$

$$-\frac{7bG_c d_t\phi_t(x,t)}{30c}-\frac{47bG_c d_b\phi_b(x,t)}{30c}+\frac{2}{5}G_c b\frac{\partial}{\partial x}w_0(x,t)-$$

(21)

$$\frac{3E_c bc}{35-35v_c^2}\frac{\partial^2}{\partial x^2}u_{0b}(x,t)+\frac{3E_c bcd_b}{70-70v_c^2}\frac{\partial^2}{\partial x^2}\phi_b(x,t)-E_b d_b\frac{\partial^2}{\partial x^2}u_{0b}(x,t)-$$

$$E_b\frac{d_b^2}{4}\frac{\partial^2}{\partial x^2}\phi_b(x,t)+\frac{2}{5}\frac{E_c bv_c}{1-v_c^2}\frac{\partial}{\partial x}w_0(x,t)-\frac{11E_c bv_c}{30-30v_c^2}\frac{\partial}{\partial x}w_b(x,t)$$

$$+\frac{19G_c b}{30}\frac{\partial}{\partial x}w_b(x,t)-\frac{1}{30}G_c b\frac{\partial}{\partial x}w_t(x,t)-\frac{1}{30}\frac{E_c bv_c}{1-v_c^2}\frac{\partial}{\partial x}w_t(x,t)$$

$$+\frac{m_c d_t}{140}\frac{\partial^2}{\partial t^2}\phi_t(x,t)-32\frac{\mu_c bl^2 u_{0t}(x,t)}{c^3}+64\frac{\mu_c bl^2 u_{0b}(x,t)}{c^3}-$$

$$32\frac{\mu_c bl^2 u_0(x,t)}{c^3}-4\frac{\mu_c bl^2}{c^2}\frac{\partial}{\partial x}w_t(x,t)-32\frac{\mu_c bl^2 d_b\phi_b(x,t)}{c^3}+$$

$$\frac{7\mu_c bl^2}{15c}\frac{\partial^2}{\partial x^2}u_{0t}(x,t)-12\frac{\mu_c bl^2}{c^2}\frac{\partial}{\partial x}w_b(x,t)-16\frac{\mu_c bl^2 d_t\phi_t(x,t)}{c^3}$$

$$-\frac{47\mu_c bl^2}{15c}\frac{\partial^2}{\partial x^2}u_{0b}(x,t)+\frac{47\mu_c bl^2 d_b}{30c}\frac{\partial^2}{\partial x^2}\phi_b(x,t)+\frac{8}{3}\frac{\mu_c bl^2}{c}\frac{\partial^2}{\partial x^2}u_0(x,t)$$

$$-48\frac{\mu_c bl^2 u_1(x,t)}{c^2}+16\frac{\mu_c bl^2}{c^2}\frac{\partial}{\partial x}w_0(x,t)+\frac{7\mu_c bl^2 d_t}{30c}\frac{\partial^2}{\partial x^2}\phi_t(x,t)$$

$$+\frac{4}{5}\mu_c bl^2\frac{\partial^2}{\partial x^2}u_1(x,t)+\frac{2}{5}\mu_c bl^2\frac{\partial^3}{\partial x^3}w_0(x,t)-\frac{1}{30}\mu_c bl^2\frac{\partial^3}{\partial x^3}w_t(x,t)=0$$

(21)

$$\delta\phi_t: -\frac{m_c cd_t}{140}\frac{\partial^2}{\partial t^2}u_1(x,t)-\frac{m_c d_b d_t}{280}\frac{\partial^2}{\partial t^2}\phi_b(x,t)+\frac{3m_c d_t^2}{140}\frac{\partial^2}{\partial t^2}\phi_t(x,t)$$

$$+\frac{1}{30}m_c d_t\frac{\partial^2}{\partial t^2}u_0(x,t)-\frac{4}{3}\frac{bd_t G_c u_0(x,t)}{c}+\frac{2}{5}bd_t G_c u_1(x,t)+$$

$$\frac{E_c bc^2 d_t}{140-140v_c^2}\frac{\partial^2}{\partial x^2}u_1(x,t)+\frac{7bd_t G_c d_b\phi_b(x,t)}{60c}+\frac{1}{12}m_t d_t^2\frac{\partial^2}{\partial t^2}\phi_t(x,t)$$

$$+\frac{47bd_t G_c u_{0t}(x,t)}{30c}-\frac{E_c bcd_t}{140-140v_c^2}\frac{\partial^2}{\partial x^2}u_{0b}(x,t)-\frac{1}{30}\frac{E_c bcd_t}{1-v_c^2}\frac{\partial^2}{\partial x^2}u_0(x,t)$$

$$+\frac{m_c d_t}{140}\frac{\partial^2}{\partial t^2}u_{0b}(x,t)+\frac{3m_c d_t}{70}\frac{\partial^2}{\partial t^2}u_{0t}(x,t)-E_t\frac{d_t^3}{12}\frac{\partial^2}{\partial x^2}\phi_t(x,t)$$

$$\frac{E_c bcd_t d_b}{280-280v_c^2}\frac{\partial^2}{\partial x^2}\phi_b(x,t)-\frac{7bd_t G_c u_{0b}(x,t)}{30c}+\frac{G_c bd_t}{60}\frac{\partial}{\partial x}w_b(x,t)+$$

$$\frac{E_c v_c bd_t}{60-60v_c^2}\frac{\partial}{\partial x}w_b(x,t)-\frac{1}{5}G_c bd_t\frac{\partial}{\partial x}w_0(x,t)-\frac{1}{5}\frac{E_c v_c bd_t}{1-v_c^2}\frac{\partial}{\partial x}w_0(x,t)$$

$$+\frac{11E_c v_c bd_t}{60-60v_c^2}\frac{\partial}{\partial x}w_t(x,t)-E_t\frac{d_t^2}{4}\frac{\partial^2}{\partial x^2}u_{0t}(x,t)$$

(22)

$$+k_s bd_t G_t\left(\phi_t(x,t)+\frac{\partial}{\partial x}w_t(x,t)\right)-\frac{3E_c bcd_t}{70-70v_c^2}\frac{\partial^2}{\partial x^2}u_{0t}(x,t)+$$

$$\frac{47bG_c d_t^2\phi_t(x,t)}{60c}-\frac{16\mu_c bl^2 d_t u_{0b}(x,t)}{c^3}-\frac{3E_c bcd_t^2}{140-140v_c^2}\frac{\partial^2}{\partial x^2}\phi_t(x,t)-\frac{19G_c bd_t}{60}\frac{\partial}{\partial x}w_t(x,t)+\frac{16\mu_c bl^2 d_t^2\phi_t(x,t)}{c^3}$$

$$+\frac{2\mu_c bl^2 d_t}{c^2}\frac{\partial}{\partial x}w_b(x,t)-\frac{8\mu_c bl^2 d_t}{c^2}\frac{\partial}{\partial x}w_0(x,t)+\frac{24\mu_c bl^2 d_t u_1(x,t)}{c^2}-\frac{19\mu_c bl^2 d_t}{60}\frac{\partial^3}{\partial x^3}w_t(x,t)+$$

$$\frac{6\mu_c bl^2 d_t}{c^2}\frac{\partial}{\partial x}w_t(x,t)-\frac{1}{4}d_t\mu_t bl^2\frac{\partial^2}{\partial x^2}\phi_t(x,t)+\frac{1}{4}d_t\mu_c bl^2\frac{\partial^3}{\partial x^3}w_t(x,t)-\frac{1}{5}\mu_c bl^2 d_t\frac{\partial^3}{\partial x^3}w_0(x,t)+$$

$$\frac{\mu_c bl^2 d_t}{60}\frac{\partial^3}{\partial x^3}w_b(x,t)-\frac{47\mu_c bl^2 d_t}{30c}\frac{\partial^2}{\partial x^2}u_{0t}(x,t)-\frac{47\mu_c bl^2 d_t^2}{60c}\frac{\partial^2}{\partial x^2}\phi_t(x,t)-\frac{7\mu_c bl^2 d_t d_b}{60c}\frac{\partial^2}{\partial x^2}\phi_b(x,t)$$

$$+\frac{8\mu_c bl^2 d_t d_b\phi_b(x,t)}{c^3}-\frac{2}{5}\mu_c bl^2 d_t\frac{\partial^2}{\partial x^2}u_1(x,t)+\frac{7\mu_c bl^2 d_t}{30c}\frac{\partial^2}{\partial x^2}u_{0b}(x,t)+\frac{4}{3}\frac{\mu_c bl^2 d_t}{c}\frac{\partial^2}{\partial x^2}u_0(x,t)$$

$$-\frac{16\mu_c bl^2 d_t u_0(x,t)}{c^3}+\frac{32\mu_c bl^2 d_t u_{0t}(x,t)}{c^3}=0$$

(22)

$$\delta\phi_b: -\frac{m_c cd_b}{140}\frac{\partial^2}{\partial t^2}u_1(x,t)-\frac{m_c d_b d_t}{280}\frac{\partial^2}{\partial t^2}\phi_t(x,t)+\frac{3m_c d_b^2}{140}\frac{\partial^2}{\partial t^2}\phi_b(x,t)\cdot$$

$$-\frac{1}{30}m_c d_b\frac{\partial^2}{\partial t^2}u_0(x,t)+\frac{4}{3}\frac{bd_b Gcu_0(x,t)}{c}$$

$$+\frac{2}{5}bd_b G_c u_1(x,t)+\frac{E_c bc^2 d_b}{140-140v_c^2}\frac{\partial^2}{\partial x^2}u_1(x,t)+\frac{47bG_c d_b^2\phi_b(x,t)}{60c}+\frac{7bd_b G_c u_{0t}(x,t)}{30c}$$

(23)

$$+\frac{E_c bcd_b}{140-140v_c^2}\frac{\partial^2}{\partial x^2}u_{0t}(x,t)+\frac{1}{30}\frac{E_c bcd_b}{1-v_c^2}\frac{\partial^2}{\partial x^2}u_0(x,t)-\frac{47bd_b G_c u_{0b}(x,t)}{30c}$$

$$-\frac{m_c d_b}{140}\frac{\partial^2}{\partial t^2}u_{0t}(x,t)-\frac{3m_c d_b}{70}\frac{\partial^2}{\partial t^2}u_{0b}(x,t)+\frac{m_b}{12}d_b^2\frac{\partial^2}{\partial t^2}\phi_b(x,t)+$$

$$\frac{E_c bcd_t d_b}{280-280v_c^2}\frac{\partial^2}{\partial x^2}\phi_t(x,t)-E_b\frac{d_b^2}{4}\frac{\partial^2}{\partial x^2}u_{0b}(x,t)+\frac{G_c bd_b}{60}\frac{\partial}{\partial x}w_t(x,t)$$

$$k_s bd_b G_b\left(\phi_b(x,t)+\frac{\partial}{\partial x}w_b(x,t)\right)-E_b\frac{d_b^3}{12}\frac{\partial^2}{\partial x^2}\phi_b(x,t)$$

$$+\frac{E_c bv_c d_b}{60-60v_c^2}\frac{\partial}{\partial x}w_t(x,t)-\frac{1}{5}G_c bd_b\frac{\partial}{\partial x}w_0(x,t)-\frac{1}{5}\frac{E_c bv_c d_b}{1-v_c^2}\frac{\partial}{\partial x}w_0(x,t)$$

$$+\frac{7G_c bd_t d_b}{60c}\phi_t(x,t)-\frac{3E_c bcd_b^2}{140-140v_c^2}\frac{\partial^2}{\partial x^2}\phi_b(x,t)-\frac{19G_c bd_b}{60}\frac{\partial}{\partial x}w_b(x,t)+$$

$$\frac{11E_c bv_c d_b}{60-60v_c^2}\frac{\partial}{\partial x}w_b(x,t)+\frac{3E_c bcd_b}{70-70v_c^2}\frac{\partial^2}{\partial x^2}u_{0b}(x,t)-8\frac{\mu_c bl^2 d_b}{c^2}\frac{\partial}{\partial x}w_0(x,t)$$

$$+24\frac{\mu_c bl^2 d_b}{c^2}u_1(x,t)+2\frac{\mu_c bl^2 d_b}{c^2}\frac{\partial}{\partial x}w_t(x,t)+16\frac{\mu_c bl^2 d_b}{c^3}u_0(x,t)+$$ (23)

$$16\frac{\mu_c bl^2 d_b}{c^3}u_{0t}(x,t)-32\frac{\mu_c bl^2 d_b}{c^3}u_{0b}(x,t)+8\frac{\mu_c bl^2 d_t d_b}{c^3}\phi_t(x,t)$$

$$-\frac{7\mu_c bl^2 d_t d_b}{60c}\frac{\partial^2}{\partial x^2}\phi_t(x,t)+\frac{1}{4}\mu_b d_b bl^2\frac{\partial^3}{\partial x^3}w_b(x,t)-\frac{2}{5}\mu_c bl^2 d_b\frac{\partial^2}{\partial x^2}u_1(x,t)$$

$$-\frac{1}{4}\mu_b d_b bl^2\frac{\partial^2}{\partial x^2}\phi_b(x,t)-\frac{1}{5}\mu_c bl^2 d_b\frac{\partial^3}{\partial x^3}w_0(x,t)-\frac{19\mu_c bl^2 d_b}{60}\frac{\partial^3}{\partial x^3}w_b(x,t)$$

$$-\frac{4}{3}\frac{\mu_c bl^2 d_b}{c}\frac{\partial^2}{\partial x^2}u_0(x,t)-\frac{47\mu_c bl^2 d_b^2}{60c}\frac{\partial^2}{\partial x^2}\phi_b(x,t)-\frac{7\mu_c bl^2 d_b}{30c}\frac{\partial^2}{\partial x^2}u_{0t}(x,t)$$

$$+\frac{47\mu_c bl^2 d_b}{30c}\frac{\partial^2}{\partial x^2}u_{0b}(x,t)+16\frac{\mu_c bl^2 d_b^2}{c^3}\phi_b(x,t)+\frac{\mu_c bl^2 d_b}{60}\frac{\partial^3}{\partial x^3}w_t(x,t)$$

$$+6\frac{\mu_c bl^2 d_b}{c^2}\frac{\partial}{\partial x}w_b(x,t)=0$$

$$\delta w_t:\frac{2}{15}m_c\frac{\partial^2}{\partial t^2}w_t(x,t)+\frac{1}{15}m_c\frac{\partial^2}{\partial t^2}w_0(x,t)-\frac{1}{30}m_c\frac{\partial^2}{\partial t^2}w_b(x,t)+m_t\frac{\partial^2}{\partial t^2}w_t(x,t)+$$

$$\frac{2}{15}bG_c c\frac{\partial}{\partial x}u_1(x,t)+\frac{2}{15}\frac{bE_c v_c c}{1-v_c^2}\frac{\partial}{\partial x}u_1(x,t)-\frac{bG_c d_b}{60}\frac{\partial}{\partial x}\phi_b(x,t)-$$

$$\frac{bE_c v_c d_b}{60-60v_c^2}\frac{\partial}{\partial x}\phi_b(x,t)-\frac{2}{3}bG_c\frac{\partial}{\partial x}u_0(x,t)-\frac{2}{3}\frac{bE_c v_c}{1-v_c^2}\frac{\partial}{\partial x}u_0(x,t)+$$

$$\frac{19bG_c}{30}\frac{\partial}{\partial x}u_{0t}(x,t)-\frac{11bE_c v_c}{30-30v_c^2}\frac{\partial}{\partial x}u_{0t}(x,t)+\frac{1}{30}bG_c\frac{\partial}{\partial x}u_{0b}(x,t)+$$

$$\frac{1}{30}\frac{bE_c v_c}{1-v_c^2}\frac{\partial}{\partial x}u_{0b}(x,t)+\frac{19bG_c d_t}{60}\frac{\partial}{\partial x}\phi_t(x,t)-\frac{11bE_c v_c d_t}{60-60v_c^2}\frac{\partial}{\partial x}\phi_t(x,t)$$

$$+\frac{1}{3c}\frac{E_c bw_b(x,t)}{1-v_c^2}-\frac{2}{15}bcG_c\frac{\partial^2}{\partial x^2}w_t(x,t)-\frac{8}{3c}\frac{E_c bw_0(x,t)}{1-v_c^2}+\frac{7}{3c}\frac{E_c bw_t(x,t)}{1-v_c^2}$$ (24)

$$+\frac{1}{30}bcG_c\frac{\partial^2}{\partial x^2}w_b(x,t)-\frac{1}{15}G_c bc\frac{\partial^2}{\partial x^2}w_0(x,t)-k_s bG_t d_t\left(\frac{\partial}{\partial x}\phi_t(x,t)+\frac{\partial^2}{\partial x^2}w_t(x,t)\right)$$

$$-\frac{\mu_c bl^2 d_b}{60}\frac{\partial^3}{\partial x^3}\phi_b(x,t)+\frac{1}{15}\mu_c bl^2 c\frac{\partial^4}{\partial x^4}w_0(x,t)-8\frac{\mu_c bl^2}{c}\frac{\partial}{\partial x}u_1(x,t)-\frac{1}{30}\mu_c bl^2 c\frac{\partial^4}{\partial x^4}w_b(x,t)$$

$$-\frac{7}{3}\frac{\mu_c bl^2}{c}\frac{\partial^2}{\partial x^2}w_t(x,t)-\frac{1}{3}\frac{\mu_c bl^2}{c}\frac{\partial^2}{\partial x^2}w_b(x,t)-6\frac{\mu_c bl^2 d_t}{c^2}\frac{\partial}{\partial x}\phi_t(x,t)-2\frac{\mu_c bl^2 d_b}{c^2}\frac{\partial}{\partial x}\phi_b(x,t)$$

$$+\frac{1}{4}\mu_t d_t bl^2\frac{\partial^4}{\partial x^4}w_t(x,t)-12\frac{\mu_c bl^2}{c^2}\frac{\partial}{\partial x}u_{0t}(x,t)-\frac{1}{4}\mu_t d_t bl^2\frac{\partial^3}{\partial x^3}\phi_t(x,t)+4\frac{\mu_c bl^2}{c^2}\frac{\partial}{\partial x}u_{0b}(x,t)$$

$$-\frac{19\mu_c bl^2}{30}\frac{\partial^3}{\partial x^3}u_{0t}(x,t)+\frac{1}{30}\mu_c bl^2\frac{\partial^3}{\partial x^3}u_{0b}(x,t)-\frac{2}{3}\mu_c bl^2\frac{\partial^3}{\partial x^3}u_0(x,t)+\frac{19\mu_c bl^2 d_t}{60}\frac{\partial^3}{\partial x^3}\phi_t(x,t)$$

$$+\frac{8}{3}\frac{\mu_c bl^2}{c}\frac{\partial^2}{\partial x^2}w_0(x,t)+\frac{2}{15}\mu_c bl^2 c\frac{\partial^3}{\partial x^3}u_1(x,t)+8\frac{\mu_c bl^2}{c^2}\frac{\partial}{\partial x}u_0(x,t)+\frac{2}{15}\mu_c bl^2 c\frac{\partial^4}{\partial x^4}w_t(x,t)=0$$

$$\delta w_b:\frac{2}{15}m_c\frac{\partial^2}{\partial t^2}w_b(x,t)+\frac{1}{15}m_c\frac{\partial^2}{\partial t^2}w_0(x,t)-\frac{1}{30}m_c\frac{\partial^2}{\partial t^2}w_t(x,t)-\frac{8}{3c}\frac{E_c bw_0(x,t)}{1-v_c^2}$$

$$+\frac{2}{3}\frac{bE_c v_c}{1-v_c^2}\frac{\partial}{\partial x}u_0(x,t)-\frac{1}{30}bG_c\frac{\partial}{\partial x}u_{0t}(x,t)-\frac{1}{30}\frac{bE_c v_c}{1-v_c^2}\frac{\partial}{\partial x}u_{0t}(x,t)+\frac{1}{3c}\frac{E_c bw_t(x,t)}{1-v_c^2}$$ (25)

$$+m_b\frac{\partial^2}{\partial t^2}w_b(x,t)-\frac{19bG_c}{30}\frac{\partial}{\partial x}u_{0b}(x,t)+\frac{11bE_c v_c}{30-30v_c^2}\frac{\partial}{\partial x}u_{0b}(x,t)+\frac{2}{3}bG_c\frac{\partial}{\partial x}u_0(x,t)$$

$$+\frac{2}{15}bG_c c\frac{\partial}{\partial x}u_1(x,t)+\frac{2}{15}\frac{bE_c v_c c}{1-v_c^2}\frac{\partial}{\partial x}u_1(x,t)-\frac{bG_c d_t}{60}\frac{\partial}{\partial x}\phi_t(x,t)-\frac{2}{15}bcG_c\frac{\partial^2}{\partial x^2}w_b(x,t)$$

$$-\frac{bE_c v_c d_t}{60-60v_c^2}\frac{\partial}{\partial x}\phi_t(x,t)+\frac{19bG_c d_b}{60}\frac{\partial}{\partial x}\phi_b(x,t)-\frac{11bE_c v_c d_b}{60-60v_c^2}\frac{\partial}{\partial x}\phi_b(x,t)+\frac{7}{3c}\frac{E_c bw_b(x,t)}{1-v_c^2}$$

$$+\frac{1}{30}bcG_c\frac{\partial^2}{\partial x^2}w_t(x,t)-\frac{1}{15}G_c bc\frac{\partial^2}{\partial x^2}w_0(x,t)-k_s bE_b d_b\left(\frac{\partial}{\partial x}\phi_b(x,t)+\frac{\partial^2}{\partial x^2}w_b(x,t)\right)$$

$$+\frac{8}{3}\frac{\mu_c bl^2}{c}\frac{\partial^2}{\partial x^2}w_0(x,t)-8\frac{\mu_c bl^2}{c}\frac{\partial}{\partial x}u_1(x,t)-2\frac{\mu_c bl^2 d_t}{c^2}\frac{\partial}{\partial x}\phi_t(x,t)+\frac{1}{4}\mu_b d_b bl^2\frac{\partial^4}{\partial x^4}w_b(x,t)$$ (25)

$$+\frac{1}{15}\mu_c bl^2 c\frac{\partial^4}{\partial x^4}w_0(x,t)-\frac{7}{3}\frac{\mu_c bl^2}{c}\frac{\partial^2}{\partial x^2}w_b(x,t)-4\frac{\mu_c bl^2}{c^2}\frac{\partial}{\partial x}u_{0t}(x,t)+12\frac{\mu_c bl^2}{c^2}\frac{\partial}{\partial x}u_{0b}(x,t)$$

$$-6\frac{\mu_c bl^2 d_b}{c^2}\frac{\partial}{\partial x}\phi_b(x,t)-\frac{1}{30}\mu_c bl^2 c\frac{\partial^4}{\partial x^4}w_t(x,t)+\frac{2}{15}\mu_c bl^2 c\frac{\partial^4}{\partial x^4}w_b(x,t)+\frac{19\mu_c bl^2 d_b}{60}\frac{\partial^3}{\partial x^3}\phi_b(x,t)$$

$$-\frac{1}{30}\mu_c bl^2\frac{\partial^3}{\partial x^3}u_{0t}(x,t)-\frac{19\mu_c bl^2}{30}\frac{\partial^3}{\partial x^3}u_{0b}(x,t)+\frac{2}{3}\mu_c bl^2\frac{\partial^3}{\partial x^3}u_0(x,t)-\frac{1}{4}\mu_b d_b bl^2\frac{\partial^3}{\partial x^3}\phi_b(x,t)$$

$$-\frac{\mu_c bl^2 d_t}{60}\frac{\partial^3}{\partial x^3}\phi_t(x,t)-\frac{1}{3}\frac{\mu_c bl^2}{c}\frac{\partial^2}{\partial x^2}w_t(x,t)-8\frac{\mu_c bl^2}{c^2}\frac{\partial}{\partial x}u_0(x,t)+\frac{2}{15}\mu_c bl^2 c\frac{\partial^3}{\partial x^3}u_1(x,t)=0$$

$$\delta w_c:\frac{1}{15}m_c\frac{\partial^2}{\partial t^2}w_b(x,t)+\frac{1}{15}m_c\frac{\partial^2}{\partial t^2}w_t(x,t)+\frac{8m_c\frac{\partial^2}{\partial t^2}w_0(x,t)}{15}+\frac{1}{5}bG_c d_b\frac{\partial}{\partial x}\phi_b(x,t)$$

$$+\frac{1}{5}\frac{E_c bv_c d_b}{1-v_c^2}\frac{\partial}{\partial x}\phi_b(x,t)-\frac{4bG_c c}{15}\frac{\partial}{\partial x}u_1(x,t)-\frac{4E_c bv_c c}{15-15v_c^2}\frac{\partial}{\partial x}u_1(x,t)$$

$$+\frac{2}{5}bG_c\frac{\partial}{\partial x}u_{0t}(x,t)+\frac{2}{5}\frac{E_c bv_c}{1-v_c^2}\frac{\partial}{\partial x}u_{0t}(x,t)-\frac{2}{5}bG_c\frac{\partial}{\partial x}u_{0b}(x,t)-\frac{2}{5}\frac{E_c bv_c}{1-v_c^2}\frac{\partial}{\partial x}u_{0b}(x,t)$$

$$\frac{1}{5}bG_c d_t\frac{\partial}{\partial x}\phi_t(x,t)+\frac{1}{5}\frac{bE_c v_c d_t}{1-v_c^2}\frac{\partial}{\partial x}\phi_t(x,t)+\frac{16E_c bw_0(x,t)}{3c}\frac{1}{1-v_c^2}-\frac{8}{3c}\frac{E_c bw_b(x,t)}{1-v_c^2}$$

$$-\frac{8}{3c}\frac{bE_c w_t(x,t)}{1-v_c^2}-\frac{1}{15}bcG_c\frac{\partial^2}{\partial x^2}w_b(x,t)-\frac{8G_c bc\frac{\partial^2}{\partial x^2}w_0(x,t)}{15}-\frac{1}{15}bcG_c\frac{\partial^2}{\partial x^2}w_t(x,t)$$ (26)

$$+\frac{1}{15}\mu_c bl^2 c\frac{\partial^4}{\partial x^4}w_t(x,t)+\frac{2}{15}\mu_c bl^2\frac{\partial^3}{\partial x^3}u_{0t}(x,t)+16\frac{\mu_c bl^2\frac{\partial}{\partial x}u_1(x,t)}{c}+\frac{1}{5}\mu_c bl^2 d_t\frac{\partial^3}{\partial x^3}\phi_t(x,t)$$

$$+\frac{1}{5}\mu_c bl^2 d_b\frac{\partial^3}{\partial x^3}\phi_b(x,t)+8\frac{\mu_c bl^2 d_t\frac{\partial}{\partial x}\phi_t(x,t)}{c^2}+8\frac{\mu_c bl^2 d_b\frac{\partial}{\partial x}\phi_b(x,t)}{c^2}-\frac{4\mu_c bl^2 c\frac{\partial^3}{\partial x^3}u_1(x,t)}{15}$$

$$+\frac{1}{15}\mu_c bl^2 c\frac{\partial^4}{\partial x^4}w_b(x,t)+16\frac{\mu_c bl^2\frac{\partial}{\partial x}u_{0t}(x,t)}{c^2}-16\frac{\mu_c bl^2\frac{\partial}{\partial x}u_{0b}(x,t)}{c^2}-\frac{2}{5}\mu_c bl^2\frac{\partial^3}{\partial x^3}u_{0b}(x,t)$$

$$+\frac{8}{3}\frac{\mu_c bl^2\frac{\partial^2}{\partial x^2}w_b(x,t)}{c}-\frac{16}{3}\frac{\mu_c bl^2\frac{\partial^2}{\partial x^2}w_0(x,t)}{c}+\frac{8\mu_c bl^2 c\frac{\partial^4}{\partial x^4}w_0(x,t)}{15}+\frac{8}{3}\frac{\mu_c bl^2\frac{\partial^2}{\partial x^2}w_t(x,t)}{c}=0$$

$$\delta u_0:\frac{1}{15}m_c\frac{\partial^2}{\partial t^2}u_{0t}(x,t)+\frac{1}{15}m_c\frac{\partial^2}{\partial t^2}u_{0b}(x,t)-\frac{1}{30}m_c d_b\frac{\partial^2}{\partial t^2}\phi_b(x,t)+\frac{1}{30}m_c d_t\frac{\partial^2}{\partial t^2}\phi_t(x,t)$$

$$-\frac{8E_c bc\frac{\partial^2}{\partial x^2}u_0(x,t)}{15-15v_c^2}-\frac{1}{15}\frac{E_c bc\frac{\partial^2}{\partial x^2}u_{0t}(x,t)}{1-v_c^2}+\frac{1}{30}\frac{E_c bcd_b\frac{\partial^2}{\partial x^2}\phi_b(x,t)}{1-v_c^2}-\frac{1}{30}\frac{E_c bcd_t\frac{\partial^2}{\partial x^2}\phi_t(x,t)}{1-v_c^2}$$

$$+\frac{8m_c\frac{\partial^2}{\partial t^2}u_0(x,t)}{15}+\frac{16}{3}\frac{bG_c u_0(x,t)}{c}-\frac{8}{3}\frac{bG_c u_{0b}(x,t)}{c}-\frac{1}{15}\frac{E_c bc\frac{\partial^2}{\partial x^2}u_{0b}(x,t)}{1-v_c^2}$$

$$+\frac{4}{3}\frac{bG_c d_b\phi_b(x,t)}{c}-\frac{4}{3}\frac{bG_c d_t\phi_t(x,t)}{c}+\frac{2}{3}G_c b\frac{\partial}{\partial x}w_t(x,t)+\frac{2}{3}\frac{E_c bv_c}{1-v_c^2}\frac{\partial}{\partial x}w_t(x,t)$$

$$-\frac{2}{3}G_c b\frac{\partial}{\partial x}w_b(x,t)-\frac{2}{3}\frac{E_c bv_c}{1-v_c^2}\frac{\partial}{\partial x}w_b(x,t)-\frac{8bG_c u_{0t}(x,t)}{3c}+\frac{2}{3}\mu_c bl^2\frac{\partial^3}{\partial x^3}w_t(x,t)$$ (27)

$$+\frac{8}{3}\frac{\mu_c bl^2\frac{\partial^2}{\partial x^2}u_{0t}(x,t)}{c}+\frac{8}{3}\frac{\mu_c bl^2\frac{\partial^2}{\partial x^2}u_{0b}(x,t)}{c}-\frac{16}{3}\frac{\mu_c bl^2\frac{\partial^2}{\partial x^2}u_0(x,t)}{c}-8\frac{\mu_c bl^2\frac{\partial}{\partial x}w_t(x,t)}{c^2}$$

$$+\frac{4}{3}\frac{\mu_c bl^2 d_t\frac{\partial^2}{\partial x^2}\phi_t(x,t)}{c}-\frac{4}{3}\frac{\mu_c bl^2 d_b\frac{\partial^2}{\partial x^2}\phi_b(x,t)}{c}-\frac{2}{3}\mu_c bl^2\frac{\partial^3}{\partial x^3}w_b(x,t)+8\frac{\mu_c bl^2\frac{\partial}{\partial x}w_b(x,t)}{c^2}$$

$$-32\frac{\mu_c bl^2 u_{0t}(x,t)}{c^3}-32\frac{\mu_c bl^2 u_{0b}(x,t)}{c^3}+64\frac{\mu_c bl^2 u_0(x,t)}{c^3}-16\frac{\mu_c bl^2 d_t\phi_t(x,t)}{c^3}$$

$$+16\frac{\mu_c bl^2 d_b\phi_b(x,t)}{c^3}=0$$

$$\delta u_1: -\frac{m_c d_b c}{140}\frac{\partial^2}{\partial t^2}\phi_b(x,t) + \frac{2m_c c^2}{105}\frac{\partial^2}{\partial t^2}u_1(x,t) - \frac{m_c c}{70}\frac{\partial^2}{\partial t^2}u_{0t}(x,t)$$

$$+\frac{m_c c}{70}\frac{\partial^2}{\partial t^2}u_{0b}(x,t) - \frac{E_c bc^2}{70-70v_c^2}\frac{\partial^2}{\partial x^2}u_{0b}(x,t) + \frac{E_c bc^2}{70-70v_c^2}\frac{\partial^2}{\partial x^2}u_{0t}(x,t) +$$

$$\frac{4}{5}bcG_c u_1(x,t) - \frac{2E_c bc^3}{105-105v_c^2}\frac{\partial^2}{\partial x^2}u_1(x,t) + \frac{4}{5}bG_c u_{0t}(x,t) - \frac{4}{5}bG_c u_{0b}(x,t)$$

$$-\frac{2}{15}\frac{E_c bcv_c}{1-v_c^2}\frac{\partial}{\partial x}w_t(x,t) - \frac{2}{15}bcG_c\frac{\partial}{\partial x}w_t(x,t)\frac{2}{5}bG_c d_t \phi_t(x,t) +$$

$$\frac{E_c bc^2 d_b}{140-140v_c^2}\frac{\partial^2}{\partial x^2}\phi_b(x,t) + \frac{E_c bc^2 d_t}{140-140v_c^2}\frac{\partial^2}{\partial x^2}\phi_t(x,t) + \frac{4E_c bcv_c}{15-15v_c^2}\frac{\partial}{\partial x}w_0(x,t)$$

$$+\frac{4bcG_c}{15}\frac{\partial}{\partial x}w_0(x,t) - \frac{2}{15}\frac{E_c bcv_c}{1-v_c^2}\frac{\partial}{\partial x}w_b(x,t) - \frac{2}{15}bcG_c\frac{\partial}{\partial x}w_b(x,t) \qquad (28)$$

$$-\frac{m_c cd_t}{140}\frac{\partial^2}{\partial t^2}\phi_t(x,t) + \frac{2}{5}bG_c d_b \phi_b(x,t) + \frac{4}{5}\mu_c bl^2\frac{\partial^2}{\partial x^2}u_{0b}(x,t) +$$

$$24\frac{\mu_c bl^2 d_b}{c^2}\phi_b(x,t) + 24\frac{\mu_c bl^2 d_t}{c^2}\phi_t(x,t) - 16\frac{\mu_c bl^2}{c}\frac{\partial}{\partial x}w_0(x,t) +$$

$$8\frac{\mu_c bl^2}{c}\frac{\partial}{\partial x}w_t(x,t) + 48\frac{\mu_c bl^2}{c^2}u_1(x,t) - 48\frac{\mu_c bl^2}{c^2}u_{0b}(x,t) + 48\frac{\mu_c bl^2}{c^2}u_{0t}(x,t)$$

$$-\frac{2}{15}\mu_c bl^2 c\frac{\partial^3}{\partial x^3}w_b(x,t) + 8\frac{\mu_c bl^2}{c}\frac{\partial}{\partial x}w_b(x,t) - \frac{2}{15}\mu_c bl^2 c\frac{\partial^3}{\partial x^3}w_t(x,t)$$

$$+\frac{4\mu_c bl^2 c}{15}\frac{\partial^3}{\partial x^3}w_0(x,t) - \frac{2}{5}\mu_c bl^2 d_b\frac{\partial^2}{\partial x^2}\phi_b(x,t) - \frac{2}{5}\mu_c bl^2 d_t\frac{\partial^2}{\partial x^2}\phi_t(x,t)$$

$$-\frac{4}{5}\mu_c bl^2\frac{\partial^2}{\partial x^2}u_{0t}(x,t) - \frac{4}{5}\mu_c bl^2 c\frac{\partial^2}{\partial x^2}u_1(x,t) = 0$$

Corresponding boundary conditions of this problem yield as following.

$$\frac{E_c bc}{70-70v_c^2}\frac{\partial}{\partial x}u_{0b}(x|_0^L,t) + \frac{1}{15}\frac{E_c bc}{1-v_c^2}\frac{\partial}{\partial x}u_0(x|_0^L,t) - \frac{E_c bc^2}{70-70v_c^2}\frac{\partial}{\partial x}u_1(x|_0^L,t) - \frac{E_c bcd_b}{140-140v_c^2}\frac{\partial}{\partial x}\phi_b(x|_0^L,t)$$

$$\frac{19G_c bw_t(x|_0^L,t)}{30} - \frac{11E_c bv_c w_t(x|_0^L,t)}{30-30v_c^2} + \frac{3E_c bc}{35-35v_c^2}\frac{\partial}{\partial x}u_{0t}(x|_0^L,t) + \frac{3E_c bcd_t}{70-70v_c^2}\frac{\partial}{\partial x}\phi_t(x|_0^L,t)$$

$$-\frac{1}{30}\frac{E_c bv_c w_b(x|_0^L,t)}{1-v_c^2} - \frac{1}{30}G_c bw_b(x|_0^L,t) + \frac{2}{5}\frac{E_c bv_c w_0(x|_0^L,t)}{1-v_c^2} + \frac{2}{5}G_c bw_0(x|_0^L,t)$$

$$+E_c d_t\frac{\partial}{\partial x}u_{0t}(x|_0^L,t) + E_t\frac{d_t^2}{4}\frac{\partial}{\partial x}\phi_t(x|_0^L,t) + \frac{4}{5}\mu_c bl^2\frac{\partial}{\partial x}u_1(x|_0^L,t) + \frac{2}{5}\mu_c bl^2\frac{\partial^2}{\partial x^2}w_0(x|_0^L,t)$$

$$\frac{47\mu_c bl^2 d_t}{30c}\frac{\partial}{\partial x}\phi_t(x|_0^L,t) + \frac{7\mu_c bl^2 d_b}{30c}\frac{\partial}{\partial x}\phi_b(x|_0^L,t) + \frac{19\mu_c bl^2}{30}\frac{\partial^2}{\partial x^2}w_t(x|_0^L,t)$$

$$-\frac{1}{30}\mu_c bl^2\frac{\partial^2}{\partial x^2}w_b(x|_0^L,t) + \frac{47\mu_c bl^2}{15c}\frac{\partial}{\partial x}u_{0t}(x|_0^L,t) - \frac{7\mu_c bl^2}{15c}\frac{\partial}{\partial x}u_{0b}(x|_0^L,t) - \frac{8}{3}\frac{\mu_c bl^2}{c}\frac{\partial}{\partial x}u_0(x|_0^L,t) = 0 \quad (29)$$

$OR\ \delta u_{0t} = 0$

$$\frac{1}{15}\frac{E_c bc}{1-v_c^2}\frac{\partial}{\partial x}u_0(x|_0^L,t) + \frac{E_c bc}{70-70v_c^2}\frac{\partial}{\partial x}u_{0t}(x|_0^L,t) + \frac{E_c bc^2}{70-70v_c^2}\frac{\partial}{\partial x}u_1(x|_0^L,t)$$

$$\frac{E_c bcd_t}{140-140v_c^2}\frac{\partial}{\partial x}\phi_t(x|_0^L,t) - \frac{2}{5}G_c bw_0(x|_0^L,t) + \frac{3E_c bc}{35-35v_c^2}\frac{\partial}{\partial x}u_{0b}(x|_0^L,t) -$$

$$\frac{3E_c bcd_b}{70-70v_c^2}\frac{\partial}{\partial x}\phi_b(x|_0^L,t) + \frac{11E_c bv_c w_b(x|_0^L,t)}{30-30v_c^2} + E_b d_b\frac{\partial}{\partial x}u_{0b}(x|_0^L,t) +$$

$$E_b\frac{d_b^2}{4}\frac{\partial}{\partial x}\phi_b(x|_0^L,t) - \frac{2}{5}\frac{E_c bv_c w_0(x|_0^L,t)}{1-v_c^2} - \frac{19G_c bw_0(x|_0^L,t)}{30}$$

$$+\frac{1}{30}G_c bw_t(x|_0^L,t) + \frac{1}{30}\frac{E_c bv_c w_t(x|_0^L,t)}{1-v_c^2} - \frac{7\mu_c bl^2}{15c}\frac{\partial}{\partial x}u_{0t}(x|_0^L,t)$$

$$-\frac{2}{5}\mu_c bl^2\frac{\partial^2}{\partial x^2}w_0(x|_0^L,t) + \frac{47\mu_c bl^2}{15c}\frac{\partial}{\partial x}u_{0b}(x|_0^L,t) - \frac{47\mu_c bl^2 d_b}{30c}\frac{\partial}{\partial x}\phi_b(x|_0^L,t)$$

$$-\frac{8}{3}\frac{\mu_c bl^2}{c}\frac{\partial}{\partial x}u_0(x|_0^L,t) - \frac{4}{5}\mu_c bl^2\frac{\partial}{\partial x}u_1(x|_0^L,t) - \frac{7\mu_c bl^2 d_t}{30c}\frac{\partial}{\partial x}\phi_t(x|_0^L,t)$$

$$-\frac{19\mu_c bl^2}{30}\frac{\partial^2}{\partial x^2}w_b(x|_0^L,t) + \frac{1}{30}\mu_c bl^2\frac{\partial^2}{\partial x^2}w_t(x|_0^L,t) = 0 \qquad (30)$$

$OR\ \delta u_{0b} = 0$

$$-\frac{E_c bc^2 d_t}{140-140v_c^2}\frac{\partial}{\partial x}u_1(x|_0^L,t) + \frac{E_c bcd_t}{140-140v_c^2}\frac{\partial}{\partial x}u_{0b}(x|_0^L,t) + \frac{1}{30}\frac{E_c bcd_t}{1-v_c^2}\frac{\partial}{\partial x}u_0(x|_0^L,t)$$

$$-\frac{E_c bcd_t d_b}{280-280v_c^2}\frac{\partial}{\partial x}\phi_b(x|_0^L,t) - \frac{G_c bd_t w_b(x|_0^L,t)}{60} - \frac{E_c v_c bd_t w_b(x|_0^L,t)}{60-60v_c^2} +$$

$$\frac{1}{5}\frac{E_c v_c bd_t w_0(x|_0^L,t)}{1-v_c^2} - \frac{11E_c v_c bd_t w_t(x|_0^L,t)}{60-60v_c^2} + E_t\frac{d_t^2}{4}\frac{\partial}{\partial x}u_{0t}(x|_0^L,t) +$$

$$E_t\frac{d_t^3}{12}\frac{\partial}{\partial x}\phi_t(x|_0^L,t) - k_s bG_t d_t\left(w_t(x|_0^L,t)\right) + \frac{3E_c bcd_t}{70-70v_c^2}\frac{\partial}{\partial x}u_{0t}(x|_0^L,t)$$

$$+\frac{3E_c bcd_t^2}{140-140v_c^2}\frac{\partial}{\partial x}\phi_t(x|_0^L,t) + \frac{19G_c bd_t^2 w_t(x|_0^L,t)}{60} + \frac{19\mu_c bl^2 d_t}{60}\frac{\partial^2}{\partial x^2}w_t(x|_0^L,t) \qquad (31)$$

$$+\frac{1}{4}\mu_t d_t bl^2\frac{\partial}{\partial x}\phi_t(x|_0^L,t) - \frac{1}{4}\mu_t d_t bl^2\frac{\partial^2}{\partial x^2}w_t(x|_0^L,t) + \frac{1}{5}\mu_c bl^2 d_t\frac{\partial^2}{\partial x^2}w_0(x|_0^L,t)$$

$$-\frac{\mu_c bl^2 d_t}{60}\frac{\partial^2}{\partial x^2}w_b(x|_0^L,t) - \frac{4}{3}\frac{\mu_c bl^2 d_t}{c}\frac{\partial}{\partial x}u_0(x|_0^L,t) + \frac{47\mu_c bl^2 d_t}{30c}\frac{\partial}{\partial x}u_{0t}(x|_0^L,t)$$

$$+\frac{47\mu_c bl^2 d_t^2}{60c}\frac{\partial}{\partial x}\phi_t(x|_0^L,t) + \frac{7\mu_c bl^2 d_t d_b}{60c}\frac{\partial}{\partial x}\phi_b(x|_0^L,t) - \frac{7\mu_c bl^2 d_t}{30c}\frac{\partial}{\partial x}u_{0b}(x|_0^L,t)$$

$$+\frac{2}{5}\mu_c bl^2 d_t\frac{\partial}{\partial x}u_1(x|_0^L,t) = 0$$

$OR\ \delta\phi_t = 0$

$$-\frac{E_c bc^2 d_b}{140-140v_c^2}\frac{\partial}{\partial x}u_1(x|_0^L,t) - \frac{E_c bcd_b}{140-140v_c^2}\frac{\partial}{\partial x}u_{0t}(x|_0^L,t)$$

$$-\frac{1}{30}\frac{E_c bcd_b}{1-v_c^2}\frac{\partial}{\partial x}u_0(x|_0^L,t) - \frac{E_c bcd_t d_b}{280-280v_c^2}\frac{\partial}{\partial x}\phi_t(x|_0^L,t)$$

$$+E_b\frac{d_b^2}{4}\frac{\partial}{\partial x}u_{0b}(x|_0^L,t) - k_s bG_b d_b\left(w_b(x|_0^L,t)\right) +$$

$$E_b\frac{d_b^3}{12}\frac{\partial}{\partial x}\phi_b(x|_0^L,t) - \frac{G_c bd_b w_t(x|_0^L,t)}{60} - \frac{E_c bv_c d_b w_t(x|_0^L,t)}{60-60v_c^2}$$

$$+\frac{1}{5}G_c bd_b w_0(x|_0^L,t) + \frac{1}{5}\frac{E_c bv_c d_b w_0(x|_0^L,t)}{1-v_c^2} + \frac{3E_c bcd_b^2}{140-140v_c^2}\frac{\partial}{\partial x}\phi_b(x|_0^L,t)$$

$$+\frac{19G_c bd_b w_b(x|_0^L,t)}{60} - \frac{11E_c bv_c d_b w_b(x|_0^L,t)}{60-60v_c^2} - \frac{3E_c bcd_b}{70-70v_c^2}\frac{\partial}{\partial x}u_{0b}(x|_0^L,t) \qquad (32)$$

$$+\frac{7\mu_c bl^2 d_t d_b}{60c}\frac{\partial}{\partial x}\phi_t(x|_0^L,t) - \frac{1}{4}\mu_b d_b bl^2\frac{\partial^2}{\partial x^2}w_b(x|_0^L,t) +$$

$$\frac{2}{5}\mu_c bl^2 d_b\frac{\partial}{\partial x}u_1(x|_0^L,t) + \frac{1}{4}\mu_b d_b bl^2\frac{\partial}{\partial x}\phi_b(x|_0^L,t) + \frac{1}{5}\mu_c bl^2 d_b\frac{\partial^2}{\partial x^2}w_0(x|_0^L,t)$$

$$+\frac{19\mu_c bl^2 d_b}{60}\frac{\partial^2}{\partial x^2}w_b(x|_0^L,t) + \frac{4}{3}\frac{\mu_c bl^2 d_b}{c}\frac{\partial}{\partial x}u_0(x|_0^L,t) + \frac{47\mu_c bl^2 d_b^2}{60c}\frac{\partial}{\partial x}\phi_b(x|_0^L,t)$$

$$+\frac{7\mu_c bl^2 d_b}{30c}\frac{\partial}{\partial x}u_{0t}(x|_0^L,t) - \frac{47\mu_c bl^2 d_b}{30c}\frac{\partial}{\partial x}u_{0b}(x|_0^L,t) - \frac{\mu_c bl^2 d_b}{60}\frac{\partial^2}{\partial x^2}w_t(x|_0^L,t) = 0$$

$OR\ \delta\phi_b = 0$

$$-\frac{2}{15}bG_c cu_1(x|_0^L,t) - \frac{2}{15}\frac{bE_c v_c cu_1(x|_0^L,t)}{1-v_c^2} + \frac{bG_c d_b \phi_b(x|_0^L,t)}{60} + \frac{bE_c v_c d_b \phi_b(x|_0^L,t)}{60-60v_c^2}$$

$$+\frac{2}{3}bG_c u_0(x|_0^L,t) + \frac{2}{3}\frac{bEv_c u_0(x|_0^L,t)}{1-v_c^2} - \frac{19bG_c u_{0t}(x|_0^L,t)}{30} + \frac{11bE_c v_c u_{0t}(x|_0^L,t)}{30-30v_c^2}$$

$$-\frac{1}{30}bG_c u_{0b}(x|_0^L,t) - \frac{1}{30}\frac{bE_c v_c u_{0b}(x|_0^L,t)}{1-v_c^2} - \frac{19bG_c d_t \phi_t(x|_0^L,t)}{60} + \frac{11bE_c v_c d_t \phi_t(x|_0^L,t)}{60-60v_c^2}$$

$$-\frac{1}{30}bcG_c\frac{\partial}{\partial x}w_b(x|_0^L,t) + \frac{1}{15}G_c bc\frac{\partial}{\partial x}w_0(x|_0^L,t) + k_s bG_t d_t\left(\phi_t(x|_0^L,t) + \frac{\partial}{\partial x}w_t(x|_0^L,t)\right)$$

$$+\frac{\mu_c bl^2}{60}\frac{\partial^2}{\partial x^2}\phi_b(x|_0^L,t) - \frac{1}{15}\mu_c bl^2 c\frac{\partial^3}{\partial x^3}w_0(x|_0^L,t) + 8\frac{\mu_c bl^2 u_1(x|_0^L,t)}{c} + \frac{1}{30}\mu_c bl^2 c\frac{\partial^3}{\partial x^3}w_b(x|_0^L,t) \qquad (33)$$

$$+\frac{7}{3}\frac{\mu_c bl^2}{c}\frac{\partial^2}{\partial x^2}w_t(x|_0^L,t) + \frac{1}{3}\frac{\mu_c bl^2}{c}\frac{\partial}{\partial x}w_b(x|_0^L,t) + 6\frac{\mu_c bl^2 d_t \phi_t(x|_0^L,t)}{c^2} + 2\frac{\mu_c bl^2 d_b \phi_b(x|_0^L,t)}{c^2}$$

$$-\frac{1}{4}\mu_t d_t bl^2\frac{\partial^3}{\partial x^3}w_t(x|_0^L,t) + 12\frac{\mu_c bl^2 u_{0t}(x|_0^L,t)}{c^2} + \frac{1}{4}\mu_t d_t bl^2\frac{\partial^2}{\partial x^2}\phi_t(x|_0^L,t) - 4\frac{\mu_c bl^2 u_{0b}(x|_0^L,t)}{c^2}$$

$$-\frac{19\mu_c bl^2}{60}\frac{\partial^2}{\partial x^2}u_{0t}(x|_0^L,t) - \frac{1}{30}\mu_c bl^2\frac{\partial^2}{\partial x^2}u_{0b}(x|_0^L,t) + \frac{2}{3}\mu_c bl^2\frac{\partial^2}{\partial x^2}u_0(x|_0^L,t) - \frac{19\mu_c bl^2 d_t}{60}\frac{\partial^2}{\partial x^2}\phi_t(x|_0^L,t)$$

$$-\frac{8}{3}\frac{\mu_c bl^2}{c}\frac{\partial}{\partial x}w_0(x|_0^L,t) - \frac{2}{15}\mu_c bl^2 c\frac{\partial^2}{\partial x^2}u_1(x|_0^L,t) - 8\frac{\mu_c bl^2 u_0(x|_0^L,t)}{c^2} - \frac{2}{15}\mu_c bl^2 c\frac{\partial^3}{\partial x^3}w_t(x|_0^L,t)$$

$$+\frac{2}{15}bcG_c\frac{\partial}{\partial x}w_t\left(x\big|_0^L,t\right)=0$$
$$OR \quad \delta w_t=0 \tag{33}$$

$$-\frac{\mu_c bl\,d_b}{60}\frac{\partial}{\partial x}\phi_b\left(x\big|_0^L,t\right)+\frac{1}{15}\mu_c bl^2 c\frac{\partial^2}{\partial x^2}w_0\left(x\big|_0^L,t\right)-\frac{1}{30}\mu_c bl^2 c\frac{\partial^2}{\partial x^2}w_b\left(x\big|_0^L,t\right)$$
$$+\frac{1}{4}\mu_t d_t bl_2^2\frac{\partial^2}{\partial x^2}w_t\left(x\big|_0^L,t\right)-\frac{1}{4}\mu_t d_t bl^2\frac{\partial}{\partial x}\phi_t\left(x\big|_0^L,t\right)+\frac{19\mu_c bl^2}{30}\frac{\partial}{\partial x}u_{ot}\left(x\big|_0^L,t\right)$$
$$+\frac{1}{30}\mu_c bl^2\frac{\partial}{\partial x}u_{ob}\left(x\big|_0^L,t\right)-\frac{2}{3}\mu_c bl^2\frac{\partial}{\partial x}u_0\left(x\big|_0^L,t\right)+\frac{19\mu_c bl^2 d_t}{60}\frac{\partial}{\partial x}\phi_t\left(x\big|_0^L,t\right)$$
$$+\frac{2}{15}\mu_c bl^2 c\frac{\partial}{\partial x}u_1\left(x\big|_0^L,t\right)+\frac{2}{15}\mu_c bl^2 c\frac{\partial^2}{\partial x^2}w_t\left(x\big|_0^L,t\right)=0$$
$$OR \quad \frac{\partial\delta w_t}{\partial x}=0 \tag{34}$$

$$-\frac{2}{3}\frac{bE_c v_c u_0\left(x\big|_0^L,t\right)}{1-v_c^2}+\frac{1}{30}bG_c u_{0t}\left(x\big|_0^L,t\right)+\frac{1}{30}\frac{bE_c v_c u_{0t}\left(x\big|_0^L,t\right)}{1-v_c^2}$$
$$+\frac{19bG_c u_{0b}\left(x\big|_0^L,t\right)}{30}-\frac{11bE_c v_c u_{0b}\left(x\big|_0^L,t\right)}{30-30v_c^2}-\frac{2}{3}bG_c u_0\left(x\big|_0^L,t\right)$$
$$-\frac{2}{15}bG_c cu_1\left(x\big|_0^L,t\right)-\frac{2}{15}\frac{bE_c v_c cu_1\left(x\big|_0^L,t\right)}{1-v_c^2}+\frac{bG_c d_t\phi_t\left(x\big|_0^L,t\right)}{60}$$
$$+\frac{2}{15}bcG_c\frac{\partial}{\partial x}w_b\left(x\big|_0^L,t\right)+\frac{bE_c vd_t\phi_t\left(x\big|_0^L,t\right)}{60-60v_c^2}-\frac{19bG_c d_b\phi_b\left(x\big|_0^L,t\right)}{60}$$
$$-\frac{1}{30}bcG_c\frac{\partial}{\partial x}w_t\left(x\big|_0^L,t\right)+\frac{1}{15}G_c bc\frac{\partial}{\partial x}w_0\left(x\big|_0^L,t\right)+k_s bG_b d_b\left(\phi_b\left(x\big|_0^L,t\right)+\frac{\partial}{\partial x}w_b\left(x\big|_0^L,t\right)\right)$$
$$-\frac{8}{3}\frac{\mu_c bl^2}{c}\frac{\partial}{\partial x}w_0\left(x\big|_0^L,t\right)+8\frac{\mu_c bl\,u_1\left(x\big|_0^L,t\right)}{c}+2\frac{\mu_c bl^2 d_t\phi_t\left(x\big|_0^L,t\right)}{c^2}-\frac{1}{4}\mu_b d_b bl^2\frac{\partial^3}{\partial x^3}w_b\left(x\big|_0^L,t\right)$$
$$-\frac{1}{15}\mu_c bl^2 c\frac{\partial^3}{\partial x^3}w_0\left(x\big|_0^L,t\right)+\frac{7}{3}\frac{\mu_c bl^2}{c}\frac{\partial}{\partial x}w_b\left(x\big|_0^L,t\right)+4\frac{\mu_c bl^2 u_{0t}\left(x\big|_0^L,t\right)}{c^2}-12\frac{\mu_c bl^2 u_{0b}\left(x\big|_0^L,t\right)}{c^2}$$
$$+6\frac{\mu_c bl^2 d_b\phi_b\left(x\big|_0^L,t\right)}{c^2}+\frac{1}{30}\mu_c bl^2 c\frac{\partial^3}{\partial x^3}w_t\left(x\big|_0^L,t\right)-\frac{2}{15}\mu_c bl^2 c\frac{\partial^3}{\partial x^3}w_b\left(x\big|_0^L,t\right)-\frac{19\mu_c bl^2 d_b}{60}\frac{\partial^2}{\partial x^2}\phi_b\left(x\big|_0^L,t\right)$$
$$+\frac{1}{30}\mu_c bl^2\frac{\partial^2}{\partial x^2}u_{0t}\left(x\big|_0^L,t\right)+\frac{19\mu_c bl^2}{30}\frac{\partial^2}{\partial x^2}u_{0b}\left(x\big|_0^L,t\right)-\frac{2}{3}\mu_c bl^2\frac{\partial^2}{\partial x^2}u_0\left(x\big|_0^L,t\right)+\frac{1}{4}\mu_b d_b bl^2\frac{\partial^2}{\partial x^2}\phi_b\left(x\big|_0^L,t\right)$$
$$+\frac{\mu_c bl^2 d_t}{60}\frac{\partial^2}{\partial x^2}\phi_t\left(x\big|_0^L,t\right)+\frac{1}{3}\frac{\mu_c bl^2}{c}\frac{\partial}{\partial x}w_t\left(x\big|_0^L,t\right)+8\frac{\mu_c bl^2 u_0\left(x\big|_0^L,t\right)}{c^2}-\frac{2}{15}\mu_c bl^2 c\frac{\partial^2}{\partial x^2}u_1\left(x\big|_0^L,t\right)$$
$$+\frac{11bE_c v_c d_b\phi_b\left(x\big|_0^L,t\right)}{60-60v_c^2}=0$$
$$OR \quad \delta w_b=0 \tag{35}$$

$$+\frac{1}{4}\mu_b d_b bl^2\frac{\partial^2}{\partial x^2}w_b\left(x\big|_0^L,t\right)+\frac{1}{15}\mu_c bl^2 c\frac{\partial^2}{\partial x^2}w_0\left(x\big|_0^L,t\right)-\frac{1}{30}\mu_c bl^2 c\frac{\partial^2}{\partial x^2}w_t\left(x\big|_0^L,t\right)$$
$$+\frac{2}{15}\mu_c bl^2 c\frac{\partial^2}{\partial x^2}w_b\left(x\big|_0^L,t\right)+\frac{19\mu_c bl^2 d_b}{60}\frac{\partial}{\partial x}\phi_b\left(x\big|_0^L,t\right)-\frac{1}{30}\mu_c bl^2\frac{\partial}{\partial x}u_{0t}\left(x\big|_0^L,t\right)$$
$$-\frac{19\mu_c bl^2}{30}\frac{\partial}{\partial x}u_{0b}\left(x\big|_0^L,t\right)+\frac{2}{3}\mu_c bl^2\frac{\partial}{\partial x}u_0\left(x\big|_0^L,t\right)-\frac{1}{4}\mu_b d_b bl^2\frac{\partial}{\partial x}\phi_b\left(x\big|_0^L,t\right)$$
$$-\frac{\mu_c bl^2 d_t}{60}\frac{\partial}{\partial x}\phi_t\left(x\big|_0^L,t\right)+\frac{2}{15}\mu_c bl^2 c\frac{\partial}{\partial x}u_1\left(x\big|_0^L,t\right)=0$$
$$OR \quad \frac{\partial\delta w_b}{\partial x}=0 \tag{36}$$

$$-\frac{1}{5}bG_c d_b\phi_b(x,t)-\frac{1}{5}\frac{E_c bv_c d_b\phi_b(x,t)}{1-v_c^2}+\frac{4bG_c u_1(x,t)}{15}+\frac{4E_c bv_c u_1(x,t)}{15-15v_c^2}$$
$$-\frac{2}{5}bG_c u_{0t}\left(x\big|_0^L,t\right)-\frac{2}{5}\frac{E_c bv_c u_{0t}\left(x\big|_0^L,t\right)}{1-v_c^2}+\frac{2}{5}bG_c u_{0b}\left(x\big|_0^L,t\right)+\frac{2}{5}\frac{E_c bv_c u_{0b}\left(x\big|_0^L,t\right)}{1-v_c^2}$$
$$-\frac{1}{5}\frac{bE_c v_c d_t\phi_t\left(x\big|_0^L,t\right)}{1-v_c^2}-\frac{1}{5}bG_c d_t\phi_t\left(x\big|_0^L,t\right)+\frac{1}{15}bcG_c\frac{\partial}{\partial x}w_b\left(x\big|_0^L,t\right)+\frac{8G_c bc}{15}\frac{\partial}{\partial x}w_0\left(x\big|_0^L,t\right)$$
$$+\frac{1}{15}bcG_c\frac{\partial}{\partial x}w_t\left(x\big|_0^L,t\right)-\frac{1}{15}\mu_c bl^2 c\frac{\partial^3}{\partial x^3}w_t\left(x\big|_0^L,t\right)-\frac{2}{5}\mu_c bl^2\frac{\partial^2}{\partial x^2}u_{0t}\left(x\big|_0^L,t\right)-16\frac{\mu_c bl^2 u_1\left(x\big|_0^L,t\right)}{c}$$
$$-\frac{1}{5}\mu_c bl^2 d_b\frac{\partial^2}{\partial x^2}\phi_b\left(x\big|_0^L,t\right)-8\frac{\mu_c bl^2 d_t\phi_t\left(x\big|_0^L,t\right)}{c^2}-8\frac{\mu_c bl^2 d_b\phi_b\left(x\big|_0^L,t\right)}{c^2}+\frac{4\mu_c bl^2 c}{15}\frac{\partial^2}{\partial x^2}u_1\left(x\big|_0^L,t\right)$$
$$-\frac{1}{15}\mu_c bl^2 c\frac{\partial^3}{\partial x^3}w_b\left(x\big|_0^L,t\right)-16\frac{\mu_c bl^2 u_{0t}\left(x\big|_0^L,t\right)}{c^2}+16\frac{\mu_c bl^2 u_{0b}\left(x\big|_0^L,t\right)}{c^2}+\frac{2}{5}\mu_c bl^2\frac{\partial^2}{\partial x^2}u_{0b}\left(x\big|_0^L,t\right)$$
$$-\frac{8}{3}\frac{\mu_c bl^2}{c}\frac{\partial}{\partial x}w_b\left(x\big|_0^L,t\right)+\frac{16}{3}\frac{\mu_c bl^2}{c}\frac{\partial}{\partial x}w_0\left(x\big|_0^L,t\right)-\frac{8\mu_c bl^2 c}{15}\frac{\partial^3}{\partial x^3}w_0\left(x\big|_0^L,t\right)-\frac{8}{3}\frac{\mu_c bl^2}{c}\frac{\partial}{\partial x}w_t\left(x\big|_0^L,t\right)$$
$$-\frac{1}{5}\mu_c bl^2 d_t\frac{\partial^2}{\partial x^2}\phi_t\left(x\big|_0^L,t\right)=0$$
$$OR \quad \delta w_c=0 \tag{37}$$

$$+\frac{8E_c bc}{15-15v_c^2}\frac{\partial}{\partial x}u_0\left(x\big|_0^L,t\right)+\frac{1}{15}\frac{E_c bc}{1-v_c^2}\frac{\partial}{\partial x}u_{0t}\left(x\big|_0^L,t\right)-\frac{1}{30}\frac{E_c bcd_b}{1-v_c^2}\frac{\partial}{\partial x}\phi_b\left(x\big|_0^L,t\right)+\frac{1}{30}\frac{E_c bcd_t}{1-v_c^2}\frac{\partial}{\partial x}\phi_t\left(x\big|_0^L,t\right)$$
$$+\frac{1}{15}\frac{E_c bc}{1-v_c^2}\frac{\partial}{\partial x}u_{0b}\left(x\big|_0^L,t\right)-\frac{2}{3}G_c bw_t\left(x\big|_0^L,t\right)-\frac{2}{3}\frac{E_c bv_c w_t\left(x\big|_0^L,t\right)}{1-v_c^2}+\frac{2}{3}G_c bw_b\left(x\big|_0^L,t\right)$$
$$+\frac{2}{3}\frac{E_c bv_c w_b\left(x\big|_0^L,t\right)}{1-v_c^2}-\frac{2}{3}\mu_c bl^2\frac{\partial^2}{\partial x^2}w_t\left(x\big|_0^L,t\right)+\frac{4}{3}\frac{\mu_c bl^2 d_b}{c}\frac{\partial}{\partial x}\phi_b\left(x\big|_0^L,t\right)+\frac{2}{3}\mu_c bl^2\frac{\partial^2}{\partial x^2}w_b\left(x\big|_0^L,t\right)$$
$$-\frac{8}{3}\frac{\mu_c bl^2}{c}\frac{\partial}{\partial x}u_{0t}\left(x\big|_0^L,t\right)-\frac{8}{3}\frac{\mu_c bl^2}{c}\frac{\partial}{\partial x}u_{0b}\left(x\big|_0^L,t\right)+\frac{16}{3}\frac{\mu_c bl^2}{c}\frac{\partial}{\partial x}u_0\left(x\big|_0^L,t\right)-\frac{4}{3}\frac{\mu_c bl^2 d_t}{c}\frac{\partial}{\partial x}\phi_t\left(x\big|_0^L,t\right)=0$$
$$OR \quad \frac{\partial\delta w_c}{\partial x}=0 \tag{38}$$

$$+\frac{E_c bc^2}{70-70v_c^2}\frac{\partial}{\partial x}u_{0b}(x,t)-\frac{E_c bc^2}{70-70v_c^2}\frac{\partial}{\partial x}u_{0t}(x,t)+\frac{2E_c bc^3}{105-105v_c^2}\frac{\partial}{\partial x}u_1(x,t)+\frac{2}{15}\frac{E_c bcv_c w_t(x,t)}{1-v_c^2}$$
$$+\frac{2}{15}bcG_c w_t(x,t)-\frac{E_c bc^2 d_b}{140-140v_c^2}\frac{\partial}{\partial x}\phi_b(x,t)-\frac{E_c bc^2 d_t}{140-140v_c^2}\frac{\partial}{\partial x}\phi_t(x,t)-\frac{4E_c bcv_c w_0(x,t)}{15-15v_c^2}$$
$$-\frac{4bcG_c w_0(x,t)}{15}+\frac{2}{15}\frac{E_c bcv_c w_b(x,t)}{1-v_c^2}+\frac{2}{15}bcG_c w_b(x,t)-\frac{4}{5}\mu_c bl^2\frac{\partial}{\partial x}u_{0b}(x,t)$$
$$+\frac{2}{15}\mu_c bl^2 c\frac{\partial^2}{\partial x^2}w_b(x,t)+\frac{2}{15}\mu_c bl^2 c\frac{\partial^2}{\partial x^2}w_t(x,t)-\frac{4\mu_c bl^2 c}{15}\frac{\partial^2}{\partial x^2}w_0(x,t)+\frac{2}{5}\mu_c bl^2 d_b\frac{\partial}{\partial x}\phi_b(x,t)$$
$$+\frac{2}{5}\mu_c bl^2 d_t\frac{\partial}{\partial x}\phi_t(x,t)+\frac{4}{5}\mu_c bl^2\frac{\partial}{\partial x}u_{0t}(x,t)+\frac{4}{5}\mu_c bl^2 c\frac{\partial}{\partial x}u_1(x,t)=0$$
$$OR \quad \delta u_0=0 \tag{39}$$

$$\frac{E_c bc^2}{70-70v_c^2}\frac{\partial}{\partial x}u_{0b}(x,t)-\frac{E_c bc^2}{70-70v_c^2}\frac{\partial}{\partial x}u_{0t}(x,t)+\frac{2E_c bc^3}{105-105v_c^2}\frac{\partial}{\partial x}u_1(x,t)-\frac{E_c bc^2 db}{140-140v_c^2}\frac{\partial}{\partial x}\phi_b(x,t)$$
$$+\frac{2}{15}\frac{E_c bcv_c w_b(x,t)}{1-v_c^2}+\frac{2}{15}bcG_c w_b(x,t)+\frac{2}{15}\frac{E_c bcv_c w_t(x,t)}{1-v_c^2}+\frac{2}{15}bcG_c w_t(x,t)$$
$$-\frac{E_c bc^2 dt}{140-140v_c^2}\frac{\partial}{\partial x}\phi_t(x,t)-\frac{4E_c bcv_c w_0(x,t)}{15-15v_c^2}-\frac{4bcG_c w_0(x,t)}{15}+\frac{4}{5}\mu_c bl^2\frac{\partial}{\partial x}u_{ot}(x,t)$$
$$+\frac{2}{5}\mu_c bl^2 d_t\frac{\partial}{\partial x}\phi_t(x,t)-\frac{4}{5}\mu_c bl^2\frac{\partial}{\partial x}u_{ob}(x,t)+\frac{2}{5}\mu_c bl^2 d_b\frac{\partial}{\partial x}\phi_b(x,t)+\frac{4}{5}\mu_c bl^2 c\frac{\partial}{\partial x}u_1(x,t)$$
$$-\frac{4\mu_c bl^2 c}{15}\frac{\partial^2}{\partial x^2}w_0(x,t)+\frac{2}{15}\mu_c bl^2 c\frac{\partial^2}{\partial x^2}w_t(x,t)+\frac{2}{15}\mu_c bl^2 c\frac{\partial^2}{\partial x^2}w_b(x,t)=0$$
$$OR \quad \delta u_1=0 \tag{40}$$

4. Numerical result and discussion

4.1 Solution method

Because these analytical methods are unable to solve these equations and boundary conditions, a shooting method (launching method) is applied as the numerical method in the study. The method used is for solving boundary value differential equations that convert boundary value problems into the initial value to solve the differential equation. Using repetitive methods and adjusting the final values with predicted values in the problem improves the response (Wang *et al.* 2013, Xie and Pang 2016).

The multiple launch method is an improved method to achieve better, more accurate, and faster results. In this method, the domain of the problem (for example, the length of the beam) is divided into smaller elements. As the results show, this process does not require a large number of elements (Aziz 1975, Bock and Plitt 1984). Using the differential equations in each element and solving these equations at the desired part, the numerical values of each component are obtained (such as displacements, forces, slopes, etc.). Because corresponding equations are studied in each element, and the vector of initial guess improves in each repetition, this method does not show sensitivity to the initial estimate, and the divergence problems of the solutions in the conventional launch method have

significantly improved (Li and Zhou 2001).

The approximated length in the section of the beam is divided into n sections (not necessarily equal), and we apply Q differential equations to each of them. So, for solving NQ differential equations, NQ initial conditions in each part are necessary. The NQ initial conditions are defined as the vector ξk as follows (Bock 1983, Deuflhard and Bader 1983)

$$\xi_k = \left[\xi_{1,k}^T, \xi_{2,k}^T, ..., \xi_{N,k}^T \right]^T \qquad (41)$$

By solving the equations in the elements, the result obtained at the end of each component must be compatible with the initial condition of the next component. In the shooting method, differential equations with the corresponding boundary conditions on the left end are solved to obtain the boundaries on the other side. So, the differences between the obtained and prescribed boundaries are called right error bound (Marzulli and Gheri 1989). In the other words, the results are obtained based on the error bound, error tolerance of the problem, as the input value. Regarding the error, iterative scheme must be incorporated in the method.

4.2 Comparison study

The comparison study is performed in two steps. In the first step, classical equations with corresponding boundary conditions, $l = 0$, are considered. In the second step, the nano-scale sandwich panel is turned out into a simple one-layer beam and is compared to the nano-scale Timoshenko beam.

4.2.1 Classical approach

As mentioned before, the classical high order Timoshenko sandwich beam is compared to Euler-Bernoulli frameworks done by finite difference, finite element and experimental methods written in literature. For this work, geometrical configuration is regarded as $L = 30$ cm, $c = 3$ cm, $b = 5$ cm, and $d_s = d_t = d_b = 0.2$ cm. Material properties for the core are $E_c = 56$ Mpa, $G_c = 22$ Mpa, $\rho_c = 60$ kg/m^3 and for skins $E_s = 210$ Gpa, $v_s = 0.3$, $\rho_s = 7900$ kg/m^3. Results are represented in Table. 1 with error bound of 10^{-6} and one order of magnitude for the number of iterations.

4.2.2 Nonclassical approach

In light of the fact that stresses in the longitudinal direction of the core are given in this study, not only soft cores but also stiff cores can be regarded. For this reason, material properties of the core are evaluated as the same for skins and therefore a nano-scale sandwich beam is turned into a nano-scale simple one-layer Timoshenko beam. In this step, material properties of the core and skins are $E = 1.44$ Gpa, $\rho = 1220$ kg/m^3, $v = 0.38$, and $l = 17.6 \times 10^{-6}$ and for various values of h, L and b. Comparison results are given in Table 2 with error bound of 10^{-6} and two orders of

Table 1 A comparison on fundamental natural frequency of FSDT[9] sandwich beam (present) with EBT[10] ones

f	Experiment (Jensen and Irgens 1999)	FDM (Sokolinsky *et al.* 2002)	FEM (Khalili *et al.* 2013)	Present
1	263	245	251	257.83
2	----	521	537	544.27
3	889	856	874	882.08
4	1289	1266	1282	1291.02
5	1774	1762	1771	1779.61
6	----	2352	----	2360.56
7	----	3039	----	3027.71
8	3806	3826	----	3793.54
9	4621	4716	----	4651.56

Table 2 A comparison on fundamental natural frequency of modified FSDT sandwich beam with FSDT single layer beam

h/l	Akgöz and Civalek (2013)	Present	Akgöz and Civalek (2013)	Present	Akgöz and Civalek (2013)	Present
	$L = 10\ h$		$L = 30\ h$		$L = 100\ h$	
1	23.7053	23.7055	24.5061	24.5566	24.6045	24.6112
5	13.7192	13.6715	14.0707	14.0697	14.1128	14.1128
10	13.2748	13.2742	13.6149	13.6179	13.6555	13.7116

---

[9]First shear deformation theory
[10]Euler-Bernoulli theory

Table 3 Three mode shapes natural frequencies for soft and stiff cores under S-S and various material parameters

Core type	Soft	Stiff	Soft	Stiff	Soft	Stiff
Material parameter to skin thickness	$l/d = 2.5$		$l/d = 3$		$l/d = 3.5$	
1st mode natural frequency	0.17365	0.29178	0.12603	0.21177	0.08682	0.14588
2nd mode natural frequency	0.24847	0.74405	0.18033	0.54002	0.12423	0.37200
3rd mode natural frequency	0.28987	1.20605	0.21038	0.87533	0.14493	0.60298

Table 4 Three mode shapes natural frequencies for soft and stiff cores under S-C and various material parameters

Core type	Soft	Stiff	Soft	Stiff	Soft	Stiff
Material parameter to skin thickness	$l/d = 2.5$		$l/d = 3$		$l/d = 3.5$	
1st mode natural frequency	0.20838	0.46683	0.15124	0.33883	0.10418	0.23341
2nd mode natural frequency	0.34092	1.13671	0.24743	0.82504	0.17044	0.56835
3rd mode natural frequency	0.39929	1.83440	0.28980	1.33143	0.19963	0.91718

Table 5 Three mode shapes natural frequencies for soft and stiff cores under C-C and various material parameters

Core type	Soft	Stiff	Soft	Stiff	Soft	Stiff
Material parameter to skin thickness	$l/d = 2.5$		$l/d = 3$		$l/d = 3.5$	
1st mode natural frequency	0.26047	0.77961	0.18905	0.56585	0.13023	0.38979
2nd mode natural frequency	0.43434	1.84894	0.31524	1.34198	0.21716	0.92444
3rd mode natural frequency	0.53259	\2.96585	0.38656	2.15265	0.26629	1.48287

magnitude for the number of iterations.

5. Parametric study

In the study, the fundamental natural frequency of a nano-scale sandwich beam is scrutinized through the approach of MCST with two types of cores: soft and stiff. Skins are considered steel with material properties $E_s = 210$ Gpa, $v_s = 0.3$, $\rho_s = 7900$ kg/m^3 (Khalili *et al.* 2013). The material properties for the honeycomb soft core are given as $E_c = 56$ Mpa, $G_c = 22$ Mpa, $\rho_c = 60$ kg/m^3 (Frostig and Baruch 1994) and $E_c = 113.8$ Gpa, $v_c = 0.342$, $\rho_c = 4430$ kg/m^3 for Ti-6Al-4V stiff core (Wu *et al.* 2015). Upper and bottom face sheets have the same geometrical configurations as used in practical applications.

Numerical results are obtained by using the shooting method under three various boundary conditions: simply supported on both sides, simply supported on one side and clamped on the other, and clamped on both sides. In this way, the second statement of Eqs. (33), (35), and (37), namely $\delta w_t = 0$, $\delta w_b = 0$, $\delta w_c = 0$, and the first statement of the other boundary conditions are exploited for simply supported. In addition, the second statement of Eqs. (33), (35), and (37) and the second statement of all boundary conditions are utilized for clamped supported. All results are obtained with error bound of 10^{-6} and three orders of magnitude for the number of iterations.

In the paper, obtained frequencies ω are evaluated by $(\omega L^2 \sqrt{\rho_s/E_s})/d_s$ as dimensionless natural frequencies (frequency parameter). In the work, the first, second and
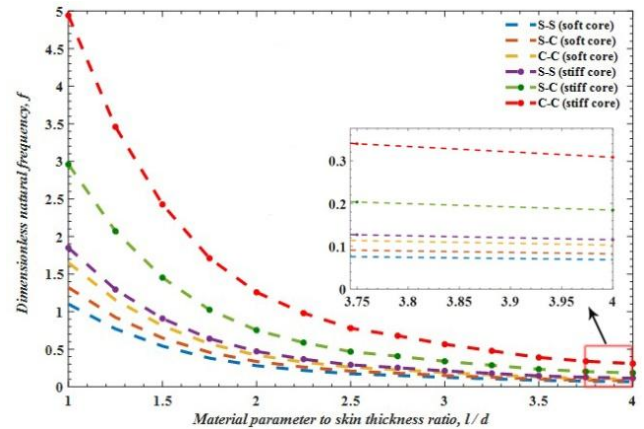

Fig. 2 Frequency parameters in terms of various material parameters for soft and stiff cores and different boundary conditions

third mode shape natural frequencies for three different material parameters and under S-S, S-C, and C-C are represented in Tables 3, 4, and 5, respectively. The first mode natural frequencies for soft and stiff cores under various boundary conditions are drawn in terms of various material size effect parameters in Fig. 2.

Tables 3, 4, and 5 and Fig. 2 are represented by geometrical configurations $L = 200 \times 10^{-12}$ m (200 nano meter), $L/C = 2$, $C/d_s = 5$, $b/d_s = 1.5$ and for given different values of l. It is observed that frequency parameters are decreased by increasing the material parameter. In other words, material stiffness of the sandwich beam is decreased by material parameter increase.

Table 6 Three mode shapes natural frequencies for soft and stiff cores under S-S and different skin thicknesses

Core type	Soft	Stiff	Soft	Stiff	Soft	Stiff
Core to skin thickness ratio	$C/d_s = 5.71$		$C/d_s = 5.41$		$C/d_s = 5.13$	
1st mode natural frequency	1.0739	1.8460	1.0203	1.8388	0.9667	1.8312
2nd mode natural frequency	1.5744	4.7210	1.5731	4.7191	1.5715	4.7172
3rd mode natural frequency	1.8373	7.6635	1.8369	7.6560	1.8366	7.6484

Table 7 Three mode shapes natural frequencies for soft and stiff cores under S-C and different skin thicknesses

Core type	Soft	Stiff	Soft	Stiff	Soft	Stiff
Core to skin thickness ratio	$C/d_s = 5.71$		$C/d_s = 5.41$		$C/d_s = 5.13$	
1st mode natural frequency	1.2930	2.9582	1.2287	2.9562	1.1641	2.9540
2nd mode natural frequency	2.1593	7.2118	2.1580	7.2092	2.1564	7.2065
3rd mode natural frequency	2.5307	11.6538	2.5304	11.6436	2.5300	11.6331

Table 8 Three mode shapes natural frequencies for soft and stiff cores under C-C and different skin thicknesses

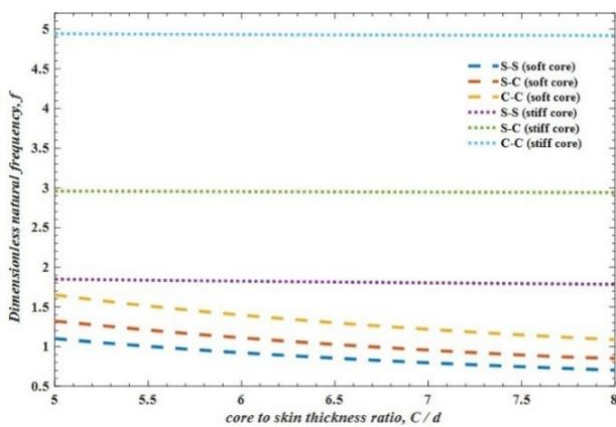| Core type	Soft	Stiff	Soft	Stiff	Soft	Stiff
Core to skin thickness ratio	$C/d_s = 5.71$		$C/d_s = 5.41$		$C/d_s = 5.13$	
1st mode natural frequency	1.6129	4.9402	1.5366	4.9370	1.4604	4.9337
2nd mode natural frequency	2.7562	11.7295	2.7522	11.7257	2.7509	11.7219
3rd mode natural frequency	3.3757	18.8372	3.3754	18.8225	3.3750	18.8073

Fig. 3 Dimensionless natural frequencies in terms of various skins thickness for soft and stiff cores and different boundary conditions

This reduction percent for all boundary conditions is the same, no matter what the type of cores. It is seen that by an increase of 400% in material parameters, there is a decrease of 94% in the first frequency parameter for this case of parametric study.

In the study, the first, second and third mode shape natural frequencies for three different skin thicknesses, and under S-S, S-C, and C-C are given in Tables 6, 7, and 8, respectively. Whereas, first mode natural frequencies for soft and stiff cores under various boundary conditions are illustrated in terms of various skin thickness in Fig. 3. All data are obtained with $l = 20$ nm, $L/l = 10$, $C/l = 5$, $b/l = 1.5$ and for given different values of d_s.

It is observed that natural frequencies increased when skin thickness increased and vice versa, while, other parameters remained constant, no matter what type of cores. However, increase percent of first natural frequencies is not the same for two types of cores. By increase of 60% in the skin thickness, 12% in the total thickness of beam, there are increments of 57%, 55% and 52% in natural frequencies for soft core, and under S-S, S-C and C-C, respectively. For stiff one, these increments are 3.6%, 0.7% and 0.5% under the same aforementioned boundary conditions, respectively.

Also, the first three modes shape natural frequencies for three different core thicknesses, and under S-S, S-C, and

Table 9 Three mode shapes natural frequencies for soft and stiff cores under S-S and different core thicknesses

Core type	Soft	Stiff	Soft	Stiff	Soft	Stiff
Core thickness to beam length ratio	$C/L = 0.55$		$C/L = 0.6$		$C/L = 0.65$	
1st mode natural frequency	1.0998	1.9005	1.0987	1.9464	1.0977	1.9878
2nd mode natural frequency	1.4736	4.8261	1.3917	4.9194	1.3247	4.9992
3rd mode natural frequency	1.7519	7.7576	1.6846	7.8522	1.6306	7.9325

Table 10 Three mode shapes natural frequencies for soft and stiff cores under S-C and different core thicknesses

Core type	Soft	Stiff	Soft	Stiff	Soft	Stiff
Core thickness to beam length ratio	$C/L = 0.55$		$C/L = 0.6$		$C/L = 0.65$	
1st mode natural frequency	1.3164	3.0058	1.3113	3.0469	1.3043	3.0831
2nd mode natural frequency	2.0560	7.3575	1.9706	7.4860	1.9003	7.5964
3rd mode natural frequency	2.4423	11.7837	2.3720	11.9144	2.3168	12.0253

Table 11 Three mode shapes natural frequencies for soft and stiff cores under C-C and different core thicknesses

Core type	Soft	Stiff	Soft	Stiff	Soft	Stiff
Core thickness to beam length ratio	$C/L = 0.55$		$C/L = 0.6$		$C/L = 0.65$	
1st mode natural frequency	1.6355	5.0007	1.6133	5.0525	1.5908	5.0986
2nd mode natural frequency	2.6556	11.939	2.5704	12.1239	2.5029	12.2826
3rd mode natural frequency	3.2908	19.0240	3.2233	19.2121	3.1704	19.3716

C-C are represented in Tables 9, 10, and 11, respectively. Nevertheless, the first mode natural frequencies for soft and stiff cores under various boundary conditions are illustrated in terms of various core thicknesses in Fig. 4. All data are
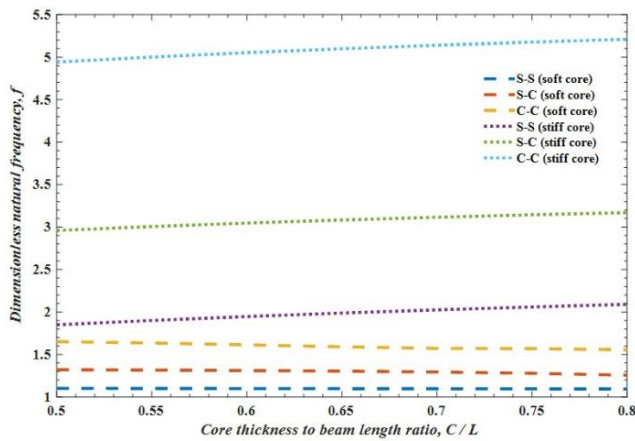

Fig. 4 Dimensionless natural frequencies in terms of various cores thickness for soft and stiff cores and various boundary conditions

obtained with $l = 20$ nm, $L/l = 10$, $d_s/l = 1$, $b/l = 1.5$ and for given different values of C.

It is concluded that natural frequencies increase for the stiff core and decrease for the soft core when core thickness increases and vice versa. With an increase of 60% in cores thickness, and 42% in the total thickness of beam, there are decreases of 0.5%, 4.8%, and 5.7% in the first natural frequencies for soft core, and under S-S, S-C and C-C, respectively. For stiff one, these increments are 13%, 7%, and 5% with the same aforementioned boundary conditions, respectively.

Moreover, the first three modes shape natural frequencies for three different sandwich beam lengths, and under S-S, S-C, and C-C are represented in Tables 12, 13, and 14, respectively. The first mode natural frequencies for soft and stiff cores under various boundary conditions are drawn in terms of various beam length in Fig. 5. All data are provided with $C = 100$ nm, $C/l = 5$, $h/l = 7$, $b/l = 1.5$ and for given different values of L.

It is mentioned that h is the total beam thickness. One can deduce that natural frequencies decrease for stiff and soft cores when beam length increases and vice versa. With an increase of 40% in beam length, there are reduction

Table 12 Three mode shapes natural frequencies for soft and stiff cores under S-S and different sandwich beam length

Core type	Soft	Stiff	Soft	Stiff	Soft	Stiff
Beam length to total beam thickness	$L/h = 1.72$		$L/h = 1.86$		$L/h = 2$	
1st mode natural frequency	0.7692	1.4317	0.6575	1.2736	0.5687	1.1400
2nd mode natural frequency	1.1667	3.7944	1.0608	3.4325	0.9800	3.1198
3rd mode natural frequency	1.3753	6.2740	1.2765	5.7287	1.2019	5.2533

Table 13 Three mode shapes natural frequencies for soft and stiff cores under S-C and different sandwich beam length

Core type	Soft	Stiff	Soft	Stiff	Soft	Stiff
Beam length to total beam thickness	$L/h = 1.72$		$L/h = 1.86$		$L/h = 2$	
1st mode natural frequency	0.9243	2.3749	0.8798	2.1494	0.7026	1.9558
2nd mode natural frequency	1.6052	5.9105	1.4525	5.3894	1.3696	4.9336
3rd mode natural frequency	1.8956	9.6969	1.7413	8.9082	1.6648	8.2114

Table 14 Three mode shapes natural frequencies for soft and stiff cores under C-C and different sandwich beam length

Core type	Soft	Stiff	Soft	Stiff	Soft	Stiff
Beam length to total beam thickness	$L/h = 1.72$		$L/h = 1.86$		$L/h = 2$	
1st mode natural frequency	1.1789	4.0194	1.0090	3.6627	0.8928	3.3559
2nd mode natural frequency	2.0579	9.6580	1.8372	8.8300	1.6941	8.1060
3rd mode natural frequency	2.5440	15.6972	2.2981	14.4325	2.1417	13.3160

amounts of 93%, 87%, and 84% in natural frequencies for soft core and S-S, S-C, and C-C, respectively and these values for the stiff core are 62%, 51%, and 47%, respectively.
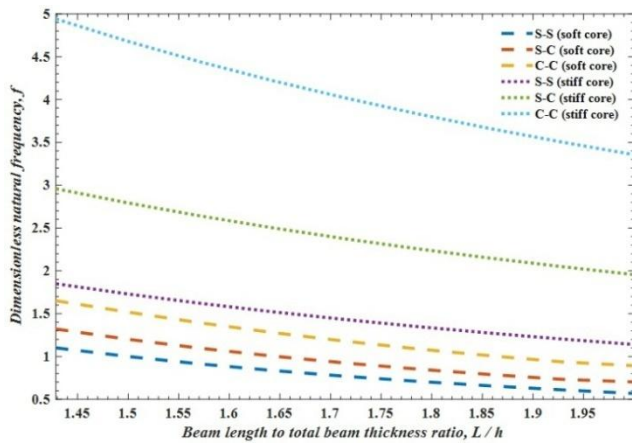

Fig. 5 Dimensionless natural frequencies in terms of deferent beam length for soft and stiff cores and various boundary conditions
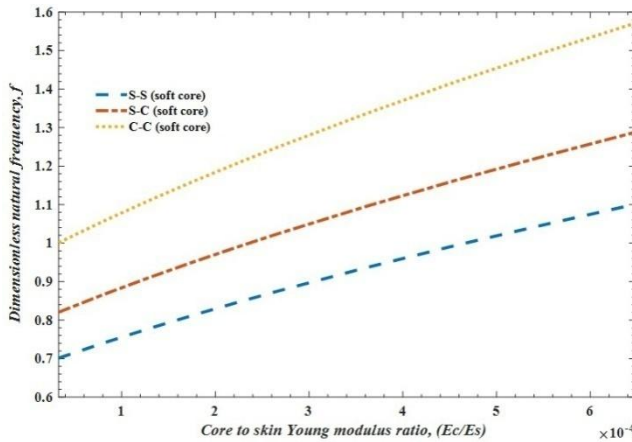
The effect of the soft-core Young modulus on the fundamental natural frequency is presented in Fig. 6. Moreover, the first three modes shape natural frequencies are given in Table 15. These results for the soft core are gained by $L = 200$ nm, $L/l = 10$, $C/l = 5$, $C/d_s = 6.35$, $b/l = 1.4$, $m_c/m_{tot} = 0.0487$, $E_c = 2.545G_c$ and for given different values of E_c. The change range of the elasticity modulus of soft cores such as honeycomb is given up to $E_c/E_s = 0.007$ (Lubin 2013). It is observed that natural frequencies increase when the soft-core Young modulus increases and vice versa. With an increase of almost 2000% in the elasticity modulus of the soft core, there are increments of 57% in the first natural frequencies regardless of type of boundary conditions. Moreover, natural frequencies increase by growth in the stiff core Young modulus and this increment is about 57% for 227% rise in the core elasticity modulus such that E_c/E_s becomes 0.5 for all three types of boundary conditions. First frequency parameters for the change in the stiff core Young modulus are illustrated in Fig. 7 and results for higher mode shapes are given in Table 16 as well. Results for the stiff core are obtained by $L = 200$ nm, $L/l = 10$, $C/l = 5$, $C/d_s = 8.33$, $b/l = 1.5$, $m_c/m_{tot} = 0.7003$, $E_c = 2.684G_c$ and for given different values of E_c.

Fig. 6 Dimensionless natural frequencies in terms of deferent soft cores Young modulus and various boundary conditions
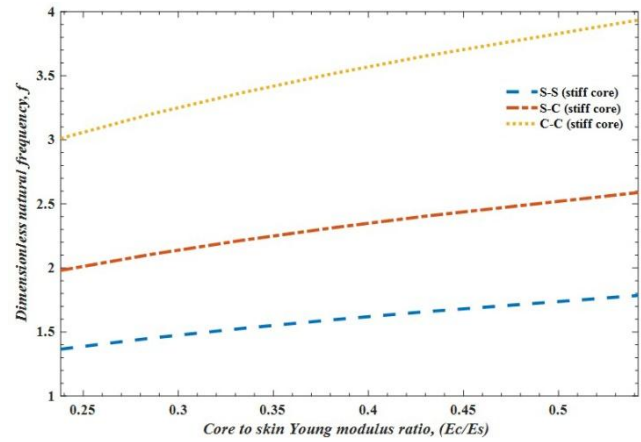

Fig. 7 Dimensionless natural frequencies in terms of deferent stiff cores Young modulus and various boundary conditions

Table 15 Three mode shapes natural frequencies for soft cores under various B.C.'s and soft core Young modulus

Core to skin Young modulus	$E_c/E_s = 0.00013$			$E_c/E_s = 0.00022$			$E_c/E_s = 0.00036$		
B.C.S's type	S-S	S-C	C-C	S-S	S-C	C-C	S-S	S-C	C-C
1st mode natural frequency	0.7772	0.9093	1.1093	0.84589	0.9897	1.2074	0.9369	1.0961	1.3373
2nd mode natural frequency	0.9773	1.3668	1.7405	1.1650	1.5760	1.9733	1.3473	1.7870	2.2219
3rd mode natural frequency	1.1247	1.5862	2.1325	1.3506	1.8374	2.4150	1.5916	2.1128	2.7379

Table 16 Three mode shapes natural frequencies for stiff cores under various B.C.'s and stiff core Young modulus

Core to skin Young modulus	$E_c/E_s = 0.24$			$E_c/E_s = 0.33$			$E_c/E_s = 0.43$		
B.C.S's type	S-S	S-C	C-C	S-S	S-C	C-C	S-S	S-C	C-C
1st mode natural frequency	1.3661	1.9809	3.0109	1.5276	2.2151	3.3669	1.6564	2.4017	3.6506
2nd mode natural frequency	3.3494	4.5957	6.8071	3.8277	5.2664	7.7907	4.2094	5.8070	8.5877
3rd mode natural frequency	5.3671	7.3298	10.7898	6.1793	8.4600	12.4341	6.8270	9.3715	13.7688

One can conclude that, in all cases, changes in skin and core thickness, beam length and material parameter result in increased frequencies for higher mode shapes regardless of cores and boundary conditions types. However, differences between results under C-C and S-C increase more than the ones under S-C and S-S boundary conditions for the stiff rather than those for flexible core.

6. Conclusions

Free vibration analysis of a nano-scale sandwich beam with two types of soft and stiff cores and isotropic, homogenous and steel skins is investigated in this paper by an extended high order theory, which has not been reported in the literature thus far. In the study, stresses in the longitudinal direction of the core, σ_{xx}, is considered, which is why stiff cores can be evaluated as well as soft cores. In our study, both HSAPT and MCST theories are examined for the core. Results reveal that obtained frequency parameters for the stiff core are more than those for the soft core. Frequency parameters for C-C are more than those for S-C, while for S-C, they are more than those for S-S boundary conditions, no matter what type of the core; however, differences between these values for the stiff core are much more than those for the soft core. Moreover, it is seen that for higher mode shapes, differences between results under C-C and S-C increase more than the ones under S-C and S-S, no matter what type of the core; however, much more differences are observed for the stiff core.

It is concluded that dimensionless natural frequencies increase by the rise in skin thickness regardless of the type of cores and boundary conditions. At the same time, the increase rate for the soft core is more than that for the stiff core. By increasing the core thickness, frequency parameters for the stiff and soft cores are increased and decreased, respectively because of material stiffness increase and decrease of the sandwich beam. This reduction for the soft core is gradual.

By an increase in beam length, fundamental natural frequencies decrease regardless of the core type and boundary conditions. However, this reduction rate is more than for the soft core. The increase effect of the core elasticity in modulus on natural frequencies growth for the stiff core is much more than that for the soft core.

References

Akgöz, B. and Civalek, Ö. (2013), "A size-dependent shear deformation beam model based on the strain gradient elasticity theory", *Int. J. Eng. Sci.*, **70**, 1-14.

Allahkarami, F., Nikkhah-Bahrami, M. and Saryazdi, M.G. (2017), "Damping and vibration analysis of viscoelastic curved microbeam reinforced with FG-CNTs resting on viscoelastic medium using strain gradient theory and DQM", *Steel Compos. Struct., Int. J.*, **25**(2), 141-155.

Ansari, R., Shojaei, M.F., Mohammadi, V., Gholami, R. and Sadeghi, F. (2014), "Nonlinear forced vibration analysis of functionally graded carbon nanotube-reinforced composite Timoshenko beams", *Compos. Struct.*, **113**, 316-327.

Asghari, M., Kahrobaiyan, M. and Ahmadian, M. (2010), "A nonlinear Timoshenko beam formulation based on the modified couple stress theory", *Int. J. Eng. Sci.*, **48**(12), 1749-1761.

Aziz, A.K. (1975), Numerical Solutions of Boundary Value Problems for Ordinary Differential Equations.

Baltacıoğlu, A., Civalek, Ö., Akgöz, B. and Demir, F. (2011), "Large deflection analysis of laminated composite plates resting on nonlinear elastic foundations by the method of discrete singular convolution", *Int. J. Press. Vessels Pip.*, **88**(8-9), 290-300.

Barretta, R., Feo, L., Luciano, R., de Sciarra, F.M. and Penna, R. (2016), "Functionally graded Timoshenko nanobeams: a novel nonlocal gradient formulation", *Compos. Part B: Eng.*, **100**, 208-219.

Bennai, R., Atmane, H.A. and Tounsi, A. (2015), "A new higher-order shear and normal deformation theory for functionally graded sandwich beams", *Steel Compos. Struct., Int. J.*, **19**(3), 521-546.

Bock, H.G. (1983), *Recent Advances in Parameteridentification Techniques for O.D.E*, Birkhäuser Boston, Boston, MA, USA.

Bock, H.G. and Plitt, K.-J. (1984), "A multiple shooting algorithm for direct solution of optimal control problems", *IFAC Proceedings Volumes*, **17**(2), 1603-1608.

Chandrashekhar, M. and Ganguli, R. (2010), "Nonlinear vibration analysis of composite laminated and sandwich plates with random material properties", *Int. J. Mech. Sci.*, **52**(7), 874-891.

Chavan, S.G. and Lal, A. (2017), "Bending behavior of SWCNT reinforced composite plates", *Steel Compos. Struct., Int. J.*, **24**(5), 537-548.

Dai, H. and Wang, X. (2006), "Non-Linear dynamic response of a single wall carbon nanotube subjected to radial impulse", *Arch. Appl. Mech.*, **76**(3-4), 145-158.

Damanpack, A. and Khalili, S. (2012), "High-order free vibration analysis of sandwich beams with a flexible core using dynamic stiffness method", *Compos. Struct.*, **94**(5), 1503-1514.

Deuflhard, P. and Bader, G. (1983), *Multiple Shooting Techniques Revisited*, Birkhäuser Boston, Boston, MA, USA.

Duan, G., Wang, X. and Jin, C. (2014), "Free vibration analysis of circular thin plates with stepped thickness by the DSC element method", *Thin-Wall. Struct.*, **85**, 25-33.

Frostig, Y. and Baruch, M. (1994), "Free Vibrations Of Sandwich Beams With A Transversely Flexible Core: A High Order Approach", *J. Sound Vib.*, **176**(2), 195-208.

Frostig, Y. and Thomsen, O.T. (2009), "On the free vibration of sandwich panels with a transversely flexible and temperature-dependent core material–Part I: Mathematical formulation", *Compos. Sci. Technol.*, **69**(6), 856-862.

Frostig, Y., Baruch, M., Vilnay, O. and Sheinman, I. (1992), "High-order theory for sandwich-beam behavior with transversely flexible core", *J. Eng. Mech.*, **118**(5), 1026-1043.

Ganapathi, M., Merzouki, T. and Polit, O. (2018), "Vibration study of curved nanobeams based on nonlocal higher-order shear deformation theory using finite element approach", *Compos. Struct.*, **184**(Supplement C), 821-838.

Gürses, M., Civalek, Ö., Korkmaz, A.K. and Ersoy, H. (2009), "Free vibration analysis of symmetric laminated skew plates by discrete singular convolution technique based on first-order shear deformation theory", *Int. J. Numer. Methods Eng.*, **79**(3), 290-313.

Hadji, L., Atmane, H.A., Tounsi, A., Mechab, I. and Bedia, E.A. (2011), "Free vibration of functionally graded sandwich plates using four-variable refined plate theory", *Appl. Math. Mech.*, **32**(7), 925-942.

He, X., Rafiee, M. and Mareishi, S. (2015), "Nonlinear dynamics of piezoelectric nanocomposite energy harvesters under parametric resonance", *Nonlinear Dyn.*, **79**(3), 1863-1880.

Heshmati, M., Yas, M.H. and Daneshmand, F. (2015), "A comprehensive study on the vibrational behavior of CNT-reinforced composite beams", *Compos. Struct.*, **125**(Supplement C), 434-448.

Jensen, A.E. and Irgens, F. (1999), "Thickness vibrations of sandwich plates and beams and delamination detection", *J. Intel. Mater Syst. Struct.*, **10**(1), 46-55.

Kahrobaiyan, M., Asghari, M., Rahaeifard, M. and Ahmadian, M. (2011), "A nonlinear strain gradient beam formulation", *Int. J.of Eng. Sci.*, **49**(11), 1256-1267.

Kar, V.R. and Panda, S.K. (2015), "Large deformation bending analysis of functionally graded spherical shell using FEM", *Struct. Eng. Mech., Int. J.*, **53**(4), 661-679.

Kavalur, P., Jeyaraj, P. and Babu, G.R. (2014), "Static behaviour of visco-elastic sandwich plate with nano-composite facings under mechanical load", *Procedia Mater. Sci.*, **5**, 1376-1384.

Khalili, S., Dehkordi, M.B., Carrera, E. and Shariyat, M. (2013), "Non-linear dynamic analysis of a sandwich beam with pseudoelastic SMA hybrid composite faces based on higher order finite element theory", *Compos. Struct.*, **96**, 243-255.

Li, S.-R. and Zhou, Y.-H. (2001), "Shooting method for non-linear vibration and thermal buckling of heated orthotropic circular plates", *J. Sound Vib.*, **248**(2), 379-386.

Lin, C.-C. and Tseng, C.-S. (1998), "Free vibration of polar orthotropic laminated circular and annular plates", *J. Sound Vib.*, **209**(5), 797-810.

Lin, F. and Xiang, Y. (2014), "Numerical analysis on nonlinear free vibration of carbon nanotube reinforced composite beams", *Int. J. Struct. Stabil. Dyn.*, **14**(01), 1350056.

Loos, M.R. and Manas-Zloczower, I. (2012), "Reinforcement efficiency of carbon nanotubes-myth and reality", *Macromol. Theory Simulat.*, **21**(2), 130-137.

Lubin, G. (2013), *Handbook of Composites*, Springer Science & Business Media.

Marshall, I., Rhodes, J. and Banks, W. (1977), "Experimental snap-buckling behaviour of thin GRP curved panels under lateral loading", *Composites*, **8**(2), 81-86.

Marzulli, P. and Gheri, G. (1989), "Estimation of the global discretization error in shooting methods for linear boundary value problems", *J. Computat. Appl. Math.*, **28**, 309-314.

McFarland, A.W. and Colton, J.S. (2005), "Role of material microstructure in plate stiffness with relevance to microcantilever sensors", *J. Micromech. Microeng.*, **15**(5), 1060.

Mehar, K., Panda, S.K., Dehengia, A. and Kar, V.R. (2016), "Vibration analysis of functionally graded carbon nanotube reinforced composite plate in thermal environment", *J. Sandw. Struct. Mater.*, **18**(2), 151-173.

Naghipour, M. and Mehrzadi, M. (2007), "Evaluation of dynamic properties of extra light weight concrete sandwich beams reinforced with CFRP", *Steel Compos. Struct., Int. J.*, **7**(6), 457-468.

Nguyen, T.-K., Nguyen, T.T.-P., Vo, T.P. and Thai, H.-T. (2015), "Vibration and buckling analysis of functionally graded sandwich beams by a new higher-order shear deformation theory", *Compos. Part B: Eng.*, **76**, 273-285.

Rahmani, O., Khalili, S., Malekzadeh, K. and Hadavinia, H. (2009), "Free vibration analysis of sandwich structures with a flexible functionally graded syntactic core", *Compos. Struct.*, **91**(2), 229-235.

Saidi, A., Baferani, A.H. and Jomehzadeh, E. (2011), "Benchmark solution for free vibration of functionally graded moderately thick annular sector plates", *Acta Mechanica*, **219**(3-4), 309-335.

Sankar, A., Natarajan, S., Haboussi, M., Ramajeyathilagam, K. and Ganapathi, M. (2014), "Panel flutter characteristics of sandwich plates with CNT reinforced facesheets using an accurate higher-order theory", *J. Fluids Struct.*, **50**, 376-391.

Shen, H.-S. and Zhu, Z. (2012), "Postbuckling of sandwich plates with nanotube-reinforced composite face sheets resting on elastic foundations", *Eur. J. Mech.-A/Solids*, **35**, 10-21.

Sokolinsky, V.S., Nutt, S.R. and Frostig, Y. (2002), "Boundary condition effects in free vibrations of higher-order soft sandwich beams", *AIAA J.*, **40**(6), 1220-1227.

Szekrényes, A. (2014), "Stress and fracture analysis in delaminated orthotropic composite plates using third-order shear deformation theory", *Appl. Math. Model.*, **38**(15-16), 3897-3916.

Tagrara, S., Benachour, A., Bouiadjra, M.B. and Tounsi, A. (2015), "On bending, buckling and vibration responses of functionally graded carbon nanotube-reinforced composite beams", *Steel Compos. Struct., Int. J.*, **19**(5), 1259-1277.

Tahouneh, V. (2017), "Vibration and mode shape analysis of sandwich panel with MWCNTs FG-reinforcement core", *Steel Compos. Struct., Int. J.*, **25**(3), 347-360.

Tong, L. (1994), "Free vibration of laminated conical shells including transverse shear deformation", *Int. J. Solids Struct.*, **31**(4), 443-456.

Tornabene, F., Fantuzzi, N., Bacciocchi, M. and Viola, E. (2016), "Effect of agglomeration on the natural frequencies of functionally graded carbon nanotube-reinforced laminated composite doubly-curved shells", *Compos. Part B: Eng.*, **89**, 187-218.

Vinson, J.R. (1999), *The Behavior of Sandwich Structures of Isotropic and Composite Materials*, Technomic Publishing Co. Inc., Lancaster, UK.

Viswanathan, K., Kim, K.S. and Lee, J.H. (2009), "Asymmetric free vibrations of laminated annular cross-ply circular plates including the effects of shear deformation and rotary inertia: spline method", *Forschung im Ingenieurwesen*, **73**(4), 205-217.

Wan, H., Delale, F. and Shen, L. (2005), "Effect of CNT length and CNT-matrix interphase in carbon nanotube (CNT) reinforced composites", *Mech. Res. Commun.*, **32**(5), 481-489.

Wang, Z.-X. and Shen, H.-S. (2012), "Nonlinear vibration and bending of sandwich plates with nanotube-reinforced composite face sheets", *Compos. Part B: Eng.*, **43**(2), 411-421.

Wang, Y.-G., Lin, W.-H. and Liu, N. (2013), "Large amplitude free vibration of size-dependent circular microplates based on the modified couple stress theory", *Int. J. Mech. Sci.*, **71**, 51-57.

Wang, Q., Shi, D., Liang, Q. and Ahad, F. (2016), "An improved Fourier series solution for the dynamic analysis of laminated composite annular, circular, and sector plate with general boundary conditions", *J. Compos. Mater.*, **50**(30), 4199-4233.

Wu, H., Kitipornchai, S. and Yang, J. (2015), "Free vibration and buckling analysis of sandwich beams with functionally graded

carbon nanotube-reinforced composite face sheets", *Int. J. Struct. Stabil. Dyn.*, **15**(7), 1540011.

Xie, W. and Pang, H. (2016), "The shooting method and integral boundary value problems of third-order differential equation", *Adv. Differ. Eq.*, **2016**(1), 138.

Xie, X., Jin, G., Ye, T. and Liu, Z. (2014), "Free vibration analysis of functionally graded conical shells and annular plates using the Haar wavelet method", *Appl. Acoustics*, **85**, 130-142.

Yang, Y., Lam, C.C., Kou, K.P. and Iu, V.P. (2014), "Free vibration analysis of the functionally graded sandwich beams by a meshfree boundary-domain integral equation method", *Compos. Struct.*, **117**(Supplement C), 32-39.

Zhang, L., Lei, Z. and Liew, K. (2015), "Computation of vibration solution for functionally graded carbon nanotube-reinforced composite thick plates resting on elastic foundations using the element-free IMLS-Ritz method", *Appl. Math. Computat.*, **256**, 488-504.

CC